Late Miocene Exhumation of Eocene and Early Miocene metamorphic Rocks in Northern Tunisia: A widespread Western Mediterranean Process Driven by Lithospheric Mantle Delamination under Foreland Thrust Belts

Guillermo Booth Rea[1,1], Seifeddine Gaidi[2,2], Fetheddine Melki[3,3], Wissem Marzougui[4,4], Patricia Ruano[5,5], Fernando Nieto[1,1], José Miguel Azañón[6,6], Jorge Pedro Galve[1,1], and Carlos Garrido[1,1]

[1]Universidad de Granada
[2]Department of Earth Sciences, Tunis El Manar University
[3]Faculty of Sciences of Tunis
[4]Office National de Mines
[5]Departamento de Geodinámica, Universidad de Granada
[6]Instituto Andaluz de Ciencias de la Tierra (C.S.I.C.-Universidad de Granada) and Departamento de Geodinámica

January 20, 2023

Abstract

Cenozoic extension in the Western Mediterranean is related to the dynamics of back-arc domains. However, extension propagated into the external Foreland Thrust Belts (FTB) of the region. Here we revisit the structure, metamorphism and radiometric ages of the Tunisian Tell FTB, where HP/LT blastomylonitic rocks (300-370ºC at 0.9-1.0 GPa), were exhumed by the sequential activity of extensional detachments. Normal faults thinning the Tunisian Tell FTB detached at two different crustal levels. The shallower one cuts down into the Atlas Mesozoic sequence, involving allochthonous Triassic evaporites at the base of the hanging-wall that form halokynetic structures intruding the Mejerda basin Late Miocene infilling. Meanwhile, the deeper-detachment level bounds metamorphic domes formed by marbles and metapsamnites. Illite crystallinity of Triassic rocks in the region shows epizonal to anchizonal values, at deep and intermediate structural depths of the Tell-Atlas FTB, respectively. New U-Pb 49.78 ± 1.28 Ma rutile ages together with existing K-Ar ages in marbles at the footwall of the deepest detachment, indicate a polymetamorphic evolution. The Tell Triassic rocks underwent Cretaceous extensional metamorphism, followed by crustal thickening and rutile growth in the Early Eocene. Further, Early Miocene thickening thrusted the metadolerites over lower-grade sediments, producing HP/LT metamorphism overprinting the base of the FTB. The exhumation of midcrustal roots of western Mediterranean FTBs after the tectonic shortening phase is a common feature of other FTB´s, like the Betics and Rif, which underwent a late-stage tearing at the edges of the subduction system together with delamination of their subcontinental lithospheric mantle.

Ichkeul blastomylonites	Ichkeul blastomylonites	Ichkeul blastomylonites	Ichkeul blastomylonites	Ichkeul blastomylonites	Ichkeul blastomylonites	Ichkeul blastomylonites	Ichkeul blastomylonites	Ichkeul blastomylonites	Ichkeul blastomylonites	Ichkeu blastomylonites
Mineral		PHENGITE	PHENGITE							
Sample	Ichkeul_-	Ichkeul_-	Ichkeul_-	Ichkeul_-	Ichkeul_-	Ichkeul_-	Ichkeul_-	Ichkeul_-	Ichkeul_-	Ichkeul_-
Analysis	ms_17	ms_55	ms_1	ms_1	ms_15	ms_47	ms_60	ms_21	ms_23	ms_35
SiO_2	48.27	47.11	46.11	46.11	46.18	47.31	47.66	45.75	47.24	46.08
TiO_2	0.61	0.06	0.01	0.01	0.14	0.05	0.11	0.15	0.06	0.07
Al_2O_3	30.41	35.37	34.25	34.25	32.77	33.05	33.17	32.32	33.43	35.20
FeO	2.99	1.56	1.95	1.95	2.88	2.15	2.04	2.37	2.04	1.59
MnO	0.01	0.00	0.00	0.00	0.02	0.00	0.00	0.01	0.01	0.00
MgO	1.88	0.26	0.67	0.67	1.03	0.88	1.08	0.96	0.67	0.44
CaO	0.08	0.14	0.21	0.21	0.52	0.24	0.49	0.66	0.11	0.24
Na_2O	0.07	0.20	0.24	0.24	0.23	0.23	0.21	0.20	0.15	0.16
K_2O	9.81	9.74	9.15	9.15	9.21	8.84	9.54	8.83	9.55	9.99
Sum.	94.12	94.44	92.59	92.59	92.96	92.76	94.30	91.26	93.25	93.77
Si	3.26	3.14	3.14	3.14	3.15	3.21	3.19	3.17	3.19	3.11
Ti	0.03	0.00	0.00	0.00	0.01	0.00	0.01	0.01	0.00	0.00
Al	2.42	2.78	2.75	2.75	2.64	2.64	2.62	2.64	2.66	2.80
Fe	0.17	0.09	0.11	0.11	0.16	0.12	0.11	0.14	0.12	0.09
Mn	0.00	0.00	0.00	0.00	0.00	0.00	0.00	0.00	0.00	0.00
Mg	0.19	0.03	0.07	0.07	0.10	0.09	0.11	0.10	0.07	0.04
Ca	0.01	0.01	0.00	0.00	0.04	0.02	0.04	0.05	0.01	0.02
Na	0.01	0.03	0.03	0.03	0.03	0.03	0.03	0.03	0.02	0.02
K	0.85	0.83	0.79	0.79	0.80	0.76	0.82	0.85	0.82	0.86
sum oct	2.07	2.03	2.03	2.03	2.07	2.06	2.04	2.05	2.07	2.04
vac	0.14	0.14	0.16	0.16	0.13	0.19	0.12	0.14	0.15	0.10
alcalin	0.86	0.86	0.84	0.84	0.87	0.81	0.88	0.86	0.85	0.90
Oxygen Sum	11.000	11.000	11.000	11.000	11.000	11.000	11.000	11.000	11.000	11.000

Hosted file

`table_s3_chlorite_tunisia.docx` available at https://authorea.com/users/539356/articles/604187-late-miocene-exhumation-of-eocene-and-early-miocene-metamorphic-rocks-in-northern-tunisia-a-widespread-western-mediterranean-process-driven-by-lithospheric-mantle-delamination-under-foreland-thrust-belts

Hosted file

`table_s4_biotite_ichkeul.docx` available at https://authorea.com/users/539356/articles/604187-late-miocene-exhumation-of-eocene-and-early-miocene-metamorphic-rocks-in-northern-tunisia-a-widespread-western-mediterranean-process-driven-by-lithospheric-mantle-delamination-under-foreland-thrust-belts

Hosted file

supporting information s1.docx available at https://authorea.com/users/539356/articles/604187-late-miocene-exhumation-of-eocene-and-early-miocene-metamorphic-rocks-in-northern-tunisia-a-widespread-western-mediterranean-process-driven-by-lithospheric-mantle-delamination-under-foreland-thrust-belts

Late Miocene Exhumation of Eocene and Early Miocene metamorphic Rocks in Northern Tunisia: A widespread Western Mediterranean Process Driven by Lithospheric Mantle Delamination under Foreland Thrust Belts

G. Booth Rea[1, 3], S. Gaidi[1, 2], F. Melki[2], W. Marzougui[4], P. Ruano[1], F. Nieto[5], J. M. Azañón[1, 3], J. P. Galvé[1]; C. J. Garrido[3]

[1]Department of Geodynamics, University of Granada, Spain. [2]Université de Tunis El Manar, Faculté des Sciences de Tunis, 1068, Tunis, Tunisia. [3]Instituto Andaluz de Ciencias de la Tierra, CSIC-UGR, Granada, Spain. [4]Office National de Mines, Tunis, Tunisia. [5]Department of Mineralogy and Petrology, University of Granada, Spain.

Corresponding author: Guillermo Booth Rea (gbooth@go.ugr.es)

Key Points:

- The Tunisian Tell Foreland Thrust Belt hosts HP/LT domes underlying Late Miocene extensional detachments driven by slab delamination.
- Metamorphic and rutile U-Pb data shows that rocks in Northern Tunisia reached epizonal conditions in the Early Eocene and Early Miocene.
- Halokinetic structures in Northern Tunisia are rooted in the Mejerda detachment and were driven by Late Miocene extension.

Abstract

Cenozoic extension in the Western Mediterranean is related to the dynamics of back-arc domains. However, extension propagated into the external Foreland Thrust Belts (FTB) of the region. Here we revisit the structure, metamorphism and radiometric ages of the Tunisian Tell FTB, where HP/LT blastomylonitic rocks (300-370ºC at 0.9-1.0 GPa), were exhumed by the sequential activity of extensional detachments. Normal faults thinning the Tunisian Tell FTB detached at two different crustal levels. The shallower one cuts down into the Atlas Mesozoic sequence, involving allochthonous Triassic evaporites at the base of the hanging-wall that form halokynetic structures intruding the Mejerda basin Late Miocene infilling. Meanwhile, the deeper-detachment level bounds metamorphic domes formed by marbles and metapsamnites. Illite crystallinity of Triassic rocks in the region shows epizonal to anchizonal values, at deep and intermediate structural depths of the Tell-Atlas FTB, respectively. New U-Pb 49.78 ± 1.28 Ma rutile ages together with existing K-Ar ages in marbles at the footwall of the deepest detachment, indicate a polymetamorphic evolution. The Tell Triassic rocks underwent Cretaceous extensional metamorphism, followed by crustal thickening and rutile growth in the Early Eocene. Further, Early Miocene thickening thrusted the metadolerites over lower-grade sediments, producing HP/LT metamorphism overprinting the base of the FTB. The exhumation of midcrustal roots of western Mediterranean FTBs after the tectonic shortening phase is a common feature of other FTB´s, like the Betics and Rif, which underwent a late-stage tearing at the edges of the subduction system together with delamination of their subcontinental lithospheric mantle.

Plain Language Summary

Orogenic arcs contain Foreland Thrust Belts (FTBs) formed by shortened sedimentary rocks. The Tell FTB in Northern Tunisia is interpreted as a classic FTB developed through protracted shortening from the Late Cretaceous until Present, formed by folded sediments and intruded by salt bodies called diapirs. However, we show here that conversely, some of the supposed diapiric bodies are metamorphic domes overlain by extensional faults, which in some case were originaly buried at depths of 25-30 km. Moreover, the remaining diapiric structures in the Tunisian Tell formed in relation to the late stage thinning and collapse of the orogenic belt, as they intrude into Late Miocene sediments. We characterize the temperature and pressure conditions reached by rocks in the domes and obtain a 49 Ma age of an early metamorphic event by radiometric dating of rutile. Other FTBs in the Western Mediterranean show similar traits, being extended after the main shortening stage and including metamorphic rocks unburied from great depths. We relate this process to delamination, a deep mantle tectonic mechanism, which strips the FTB crustal domain from its underlying mantle lithosphere. These results imply large differences in many geological features including hydrocarbon prospectivity, lithospheric structure and nature of tectonic boundaries.

1 Introduction

Certain orogenic domains of Foreland Thrust Belts (FTB´s) surrounding the western Mediterranean, in the Betics, Mallorca, Tell, Rif and Apennines occur over relatively thin continental crust and shallow LAB, below 30 and 70 km, respectively (e.g. Research group for lithospheric structure in Tunisia, 1992; Piana et al., 2002; Agostinetti et al, 2008; Miller and Agostinetti, 2012; Palomeras et al., 2014; Mancilla and Díaz, 2015; El-Sharkawy et al., 2020), in some cases contrasting with nearby domains where the crust of these FTB´s reach up to 50 km thickness, forming part of thick 150-200 km lithosphere (e.g. Mancilla et al., 2015; Li et al., 2021; El-Sharkawy et al., 2020). This feature is explained by two contrasting hypothesis, proposing either that the FTB´s preserve the original thrust stack structure with only minor, later extension, and with existing extensional structures being mostly related to Mesozoic rifting (e.g. Frizon de Lamotte et al., 1991; Gelabert et al., 1992; Platt et al., 2003; Crespo-Blanc and Frizon de Lamotte, 2006; Sabat et al., 2011; Khomsi et al., 2016; Gimeno-Vives et al., 2019; Pedrera et al., 2020). Or, alternatively, other work suggests that these FTB domains have been extended, with their lithosphere rejuvenated in relation to deep mantle tectonic mechanisms, after the thrust emplacement phase, during the Middle to Late Miocene, or younger in the Apennines-Tyrrhenian (Cohen et al., 1980; Carmignani and Kligfield, 1990; de Ruig, 1995; Crespo-Blanc and Campos, 2001; Papeschi et al., 2017; Rodríguez-Fernández et al., 2011; Booth-Rea et al., 2012; 2018; Moragues et al., 2018; 2021; de la Peña et al., 2020). Alternatively, extension affecting FTB´s in the Western Mediterranean has also been interpreted as a minor process related to the dynamics of the accretionary wedges (Jiménez-Bonilla et al., 2016; Khelil et al., 2019).

These contrasting views of the western Mediterranean FTB´s imply important differences in crustal and lithospheric structure, age of extension, hydrocarbon prospectivity, amount and age of shortening, role of tectonic inversion, age and position of orogenic boundaries and tectonic mechanisms driving deformation in the region, among other features. For example, stratigraphic omissions observed in the lithological series of these FTB domains are interpreted as related to erosion or salt welds according to the first hypothesis (e.g. Khelil et al., 2021; Daudet et al., 2020) and as extensional tectonic omissions by the later (Carmignani and Kligfield; 1990; García-Dueñas et al., 1992; Crespo-Blanc and Campos, 2001; Rodríguez-Fernández et al., 2011; Booth-Rea et al., 2012; 2018; Moragues et al., 2021). Moreover, the interpreted nature of these controversial lithological contacts will determine the maximum amount of tectonic transport across them. For example, in the Betics, interpreting these omission contacts as salt welds implies that the Numidian Flysch rocks overlying the South-Iberian passive margin sediments are autochthonous and had only minor displacement together with their underlying thrust sheet (tens of km), whilst other authors suggest hundreds of km of displacement between these different domains (Platt et al., 2003; Luján et al., 2004).

This is also the case in Northern Tunisia, where deep marine Oligocene to Early Miocene Numidian Flysch has been interpreted to have deposited directly over the previously thrusted and eroded underlying Atlas sequence, to explain the stratigraphic omissions found along its basal contact (Khomsi et al., 2021; Khomsi, Roure and Verges, 2022), whilst other authors, studying nearby outcrops in Northeastern Algeria propose their deposition over oceanic crust of the Tethys ocean (Boukaoud et al., 2021). Thus, distinguishing between extensional, stratigraphic or thrust contacts in the western Mediterranean FTB´s is key to deciphering the tectonic evolution of these regions.

Extensional fault contacts are characterized by producing lithological omissions in the stratigraphic sequence, including metamorphic gaps along crustal-scale extensional shear zones (Wernicke, 1981; Platt, 1986; Lonergan and Platt, 1995). However, given that extension cannot undo the stratigraphic and metamorphic repetitions produced by previous nappe tectonics, the extensional nature of a fault contact has to be further supported by geometrical criteria. For example, extensional faults cut down into the previous structure towards the sense of hanging-wall displacement (Wernicke and Burchfiel, 1982; Martínez-Martínez et al., 2002). The geometry of extensional systems in extended FTB´s is further determined by the rheological structure developed during the previous thrust stacking stage (e.g. Gartrell, 1997; Booth-Rea et al., 2004; Brogi, 2008). Extension with pre-rift evaporites can further promote the activity and growth of halokinetic features like diapirs, salt walls and minibasins (e.g. de Ruig, 1995; Escosa et al., 2018; Granado et al., 2021).

The Tunisian Tell and Atlas belts are generally interpreted as external FTB´s comprising only sedimentary rocks, despite the presence of the Giallo Antico marbles, well known since Roman times at the boundary between the two orogenic belts (e.g. Röder, 1988; Bugini et al., 2019). These marbles contain a WNW-ESE to WSW-ENE oriented magnetic fabric interpreted as a tectonic stretching (Ghorabi and Henry, 1992).

Equivalent marbles also crop out in Jebel Ichkeul and the Oued Belif dome, representing the structurally deepest rocks in the Tell belt (Booth-Rea et al., 2018; Khelil et al., 2019, Fig. 2). These are described as Permo-Triassic epizonal rocks that underwent temperatures between 300 and 400ºC in the core of the Oued Belif dome (Mahdi et al., 2013). These temperatures are supported by fluid inclusion studies in quartz and dolomite indicating temperatures between 220-380 ºC at minimum pressures equivalent to 6-7 km depth for the Triassic rocks (Perthuisot et al., 1978). Furthermore, at intermediate structural positions within the Tell thrust stack, metadolerites included in the Triassic evaporitic sequence show a polymetamorphic evolution, having undergone an earlier spilitic metamorphism under lower-greenschist facies, followed by a later K-Si enrichment metasomatic phase (Kurtz, 1983). This polymetamorphic evolution is constrained by K-Ar ages on K-feldspar and phlogopite in the metadolerites giving different age populations, including late Cretaceous to Paleocene ages (97-64 Ma) for samples in Le Kef diapir, younger Late Oligocene to Early Miocene (25-18 Ma) ages in more internal Triassic outcrops, and only Early Miocene ages (23-17 Ma) in the deeper Ichkeul massif (Bellon and Perthuisot, 1977), in a pattern similar to the External Rif FTB in Morocco, where Miocene metamorphism in the Temsamane nappe stack overprints older Cretaceous ages in overlying rocks (Vázquez et al., 2012; Jabaloy et al., 2015). However, this age disparity in Northern Tunisia has been interpreted as a mixture of Cretaceous ages with late Miocene magmatic related heating and thermal resetting by Bellon and Perthuisot (1977).

Interestingly, some work has shown the importance of late Miocene extension in the region related to either the internal dynamics at the deformation front of the Tell accretionary wedge (Khelil et al., 2019) or to overall Late Miocene orogenic collapse of Northern Tunisia (Cohen et al., 1980; Booth-Rea et al., 2018; 2019; 2020), which could explain the exhumation of these rocks, together with Middle Miocene granodiorites in the Oued Belief dome (e.g. Decrée et al., 2014). However, the origin, modes of exhumation, age, nature and implications that these metamorphic rocks have for the tectonic evolution of the region, and at a larger scale, for the evolution of the western Mediterranean FTB´s, have not been satisfactorily analyzed.

Here, we study the structure, metamorphism and timing of geological processes in Northwestern Tunisia using a multidisciplinary approach. We use fieldwork and the analysis of industry multichannel seismic reflection lines to study the structure of the Mejerda basin and Kroumerie massif to the Northwest, with a special emphasis in determining the relationships between polyphasic Late Miocene extension, the development of halokynetic structures, synrift basin infilling and metamorphic rocks exhumation. Moreover, we determine illite crystallinity for Triassic metapelite intercalations cropping out in the Tell FTB of Northern Tunisia and analyze the metamorphic mineral parageneses, including multiequilibrium thermobarometric results for the Ichkeul calcschist. Furthermore, we use rutile U-Pb laser ablation ion probe dating to determine the age of metamorphism in metadolerites. These data, together with other previously published K-Ar data suggest a polyphasic metamorphic evolution in the Tell-Atlas domain, between the Cretaceous and Early Miocene. These data, favor a model of Eocene to Early Miocene crustal thickening and HP/LT metamorphism followed by extensional exhumation and crustal thinning of the previous FTB, driving Late Miocene basin development, halokynessis of overthrusted evaporite-rich layers in the upper crust and ductile flow below the brittle-ductile transition. Finally, we integrate these findings in the tectonic evolution of other FTB´s of the Western Mediterranean orogenic belts.

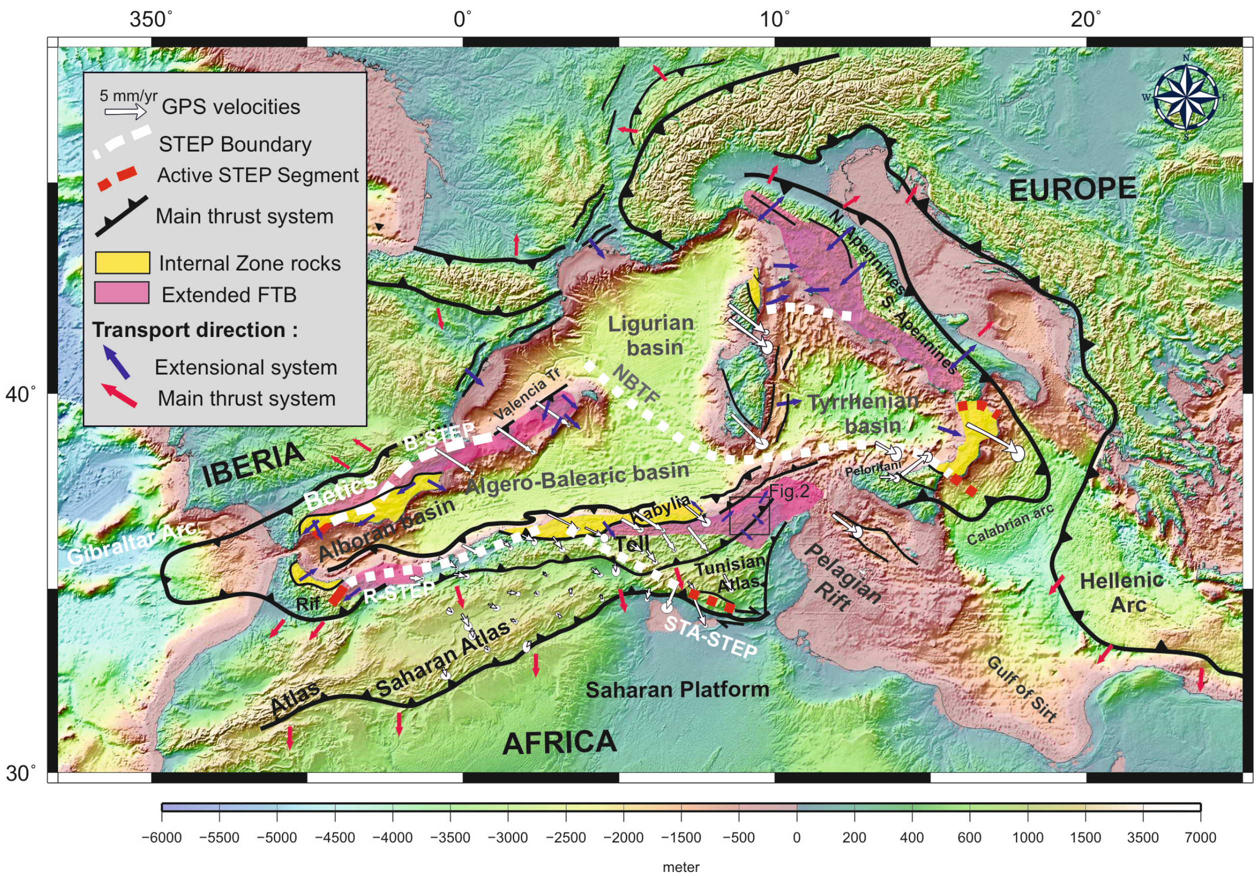

Figure 1: Tectonic boundaries, orogenic arcs and basins of the Western Mediterranean. Figure modified from Booth-Rea et al. (2007; 2018) and Gaidi et al. (2020). GPS movement towards fixed Africa from Bougrine et al. (2019) and Nocquet, (2012). Fault pattern along Algeria-Tunisia based on Kherroubi et al., (2009), Rabaute and Chamot-Rooke, (2014) and (Aïdi et al., 2018). Extended FTB domains from (Carmignani and Kligfiel, 1990), Ghisetti and Vezzani, (2002), Booth-Rea et al. (2012; 2018), Rodríguez-Fernández et al. (2013), Moragues et al., (2021).

The Tell FTB in Northern Tunisia is part of the Alpine orogenic system that surrounds the Western Mediterranean Liguro-Provencal, Algero-Balearic, Tyrrhenian and Alboran basins, formed in a context of Nubia-Eurasia convergence since Late Cretaceous time (Dewey et al., 1989). This convergent setting favored the action of other tectonic mechanisms related to subduction, like slab roll back accompanied by slab tearing and detachment at the edges of the western Mediterranean orogenic arcs, which also contributed to the development of these basins and their surrounding mountain belts (e.g. Lonergan and White, 1997; Carminati et al., 1998; Wortel and Spakman, 2000; Govers and Wortel, 2005; Booth-Rea et al., 2007; Chertova et al., 2014, van Hinsbergen et al., 2014; Romagny et al., 2020; Moragues et al., 2021). Furthermore, particularly beneath continental domains like the South Eastern Betics, Northern Tunisia, the Rif or the Central Apennines, delamination of the subcontinental lithospheric mantle driving crustal extension, magmatism and topographic uplift, has also been proposed (Duggen et al., 2003; Martínez-Martínez et al., 2006; Di Luzio et al., 2009; Roure et al., 2012; Levander et al., 2014; Mancilla et al., 2015; Petit et al., 2015; Booth-Rea et al., 2018; Camafort et al., 2020; Negredo et al., 2020) (Figure 1).

2 Geological setting

The Tell FTB in Tunisia is represented by the overthrusted nappes of the Maghrebian Tethys oceanic domain (Numidian Flysch), formed in great part by Oligocene to Early Miocene turbiditic series, and by the underlying infra-Numidian and Atlassic sedimentary series that deposited along the North Maghrebian passive margin during the Mesozoic and Cenozoic (Khomsi et al., 2009; Sami et al., 2010; Riahi et al., 2021; Belayouni, 2013)(Figure 2). The infra-Numidian domain is formed by several imbricated allochthonous nappes that include mostly Cretaceous to Aquitanian sediments (Rouvier, 1993, 1992; Khomsi et al., 2009; Belayouni et al., 2013). The infra-Numidian domain also includes Triassic evaporites, which are interpreted either as autochthonous Triassic piercing the nappe structure (Rouvier, 1992; 1993; Khelil et al., 2019) or as part of the allochthonous stratigraphic series at the base of the infra-Numidian nappes (Troudi et al., 2017; Booth-Rea et al., 2018). The autochthonous Atlas series is formed by Triassic to Oligocene sediments. The hinterland metamorphic domain of the Tell is found to the NW in the Kabylies in Algeria, where HP Eocene to Early Miocene rocks crop out (e.g. Bouillin et al., 1986; Bruguier et al., 2017), overthrusting metabasites and serpentinites attributed to the subducted Tethys oceanic crust, which represents the basement of the Numidian Flysch (e.g. Boukaoud et al., 2021). Metamorphic flysch successions also occur in la Galite island, North of Tunisia (Belayouni et al., 2010).

Northern Tunisia has been considered for decades as a paradigmatic region for the study of diapiric structures in an external foreland thrust belt context (e.g. Perthuisot, 1981; Vila, 1995; Bedir et al., 2001; Ben Chelbi et al., 2006; Melki et al., 2010; Ayed-Khaled et al., 2015; Troudi et al., 2017; Amri et al., 2020). Diapiric intrusions of Triassic evaporites are thought to have initiated in the Cretaceous during the rifting of the North Maghrebian passive margin, having been also extruded to the surface as thousand km2 large salt glaciers or canopies (Vila, 1995; Vila et al, 1996; Ghanmi et al., 2001; Masrouhi and Koyi, 2012; Masrouhi et al., 2014; Ayed-Khaled et al., 2015; Amri et al., 2020). This Mesozoic extensional-diapiric structure would have evolved later in a convergent to transcurrent setting during the Cenozoic development of the Tell and Atlas Foreland Thrust Belts (FTB) that form part of the western Mediterranean alpine orogeny (Bouaziz et al., 2002; Melki et al., 2010; 2011; Amri et al., 2020)(Figure 1). During thrusting, salt tectonics is interpreted to have played an important role, with the main decollements being located within the Triassic evaporites that presently are found at the base of the main Tellian thrust sheets (Khomsi et al., 2009, 2016; Booth-Rea et al., 2018). Thus, some authors interpret the proposed salt canopies, alternatively, as over thrusted Triassic evaporites at the base of the Tellian nappes (Khomsi et al., 2009; Troudi et al., 2017).

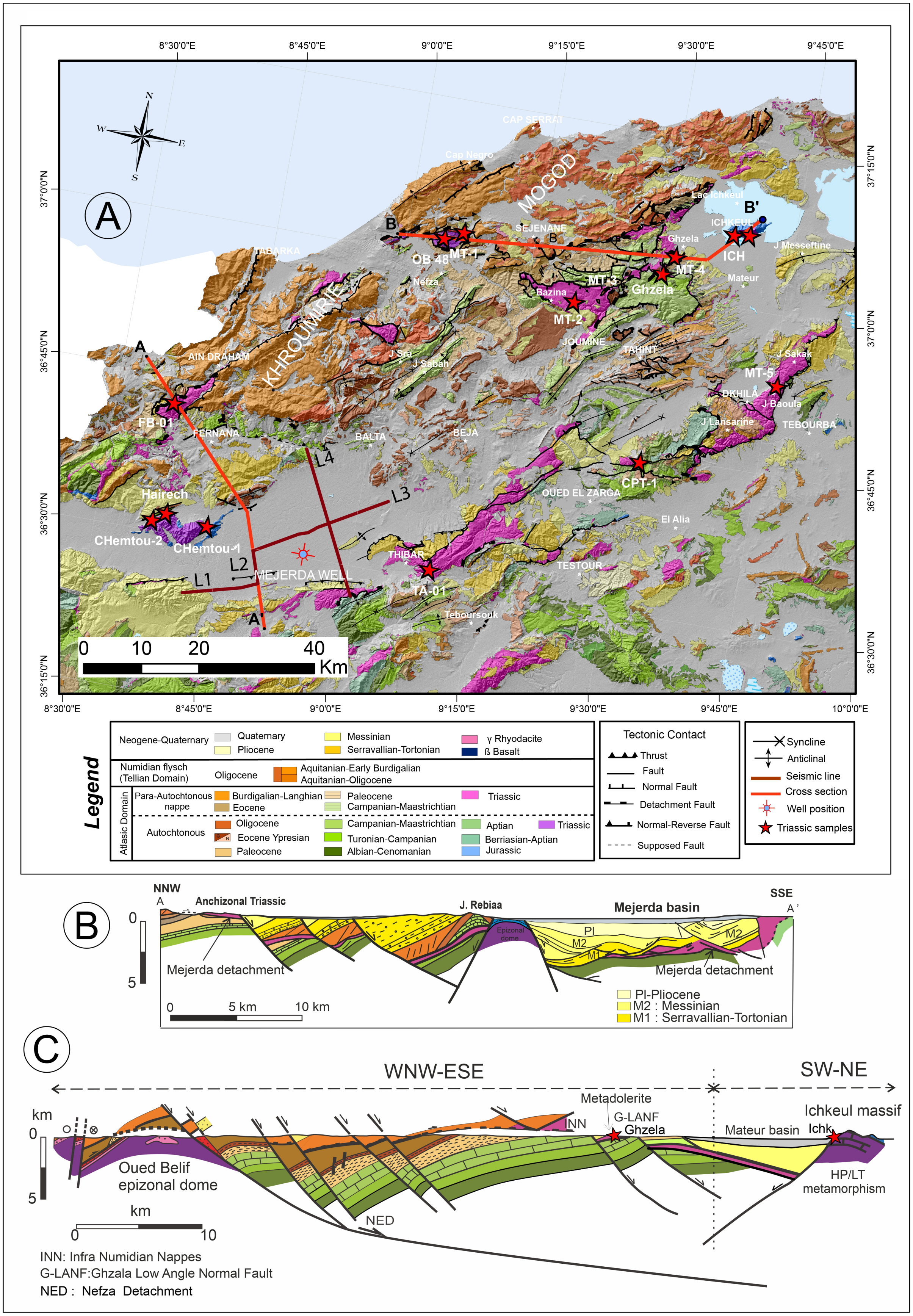

218 **Figure 2:** Geological map of Northern Tunisia and cross-sections through the studied region. a) Notice the

location of the analyzed Triassic samples together with the location of interpreted reflection seismic lines. OB 48 locality corresponds to bore hole where Mahdi et al. (2013) analyzed epizonal samples. Location in Figure 1. b) Cross section A-A´across the Kroumerie massif and the Mejerda basin. The structure across the Mejerda basin is based on reflection seismic line 2 in (a). c) Cross section B-B´ from the Oued Belief epizonal dome, through the Mogods massif, reaching the Ichkeul HP/LT massif. Notice the two extensional detachment levels, with the Ghzela LANF cutting above the Atlas Cenozoic and Cretaceous series and the Nefza detachment and associated listric fan cutting the previous structure and exhuming the Oued Belif and Ichkeul metamorphic domes.

Evidence for late Cretaceous to Palaeogene tectonic shortening is described, mostly as angular and erosive unconformities sealing folds in different regions of the Tunisian foreland basins (El Ghali et al., 2003; Masrouhi et al., 2008; Khomsi et al., 2009). During this period, special emphasis is given to a Middle to Late Eocene "Atlas event" (Frizon de Lamotte et al., 2000; Bracène and de Lamotte, 2002; Benaouali-Mebarek et al., 2006; Khomsi et al., 2009; 2021; Leprêtre et al., 2018). The Atlas event was followed by later overthrusting of Oligocene to Late Burdigalian Numidian Flysch series over Early Miocene foredeep sedimentary successions of Burdigalian to Langhian age in the Tunisian Tell (Riahi, 2010; Belayouni, 2013; Khomsi et al., 2009; 2016; Boukhalfa et al., 2020). Most authors consider shortening in Northern Tunisia continued throughout the late Miocene producing folds (Melki et al., 2010, 2011; Ramzi and Lassaad, 2017). However, recent work has reinterpreted these folds as being extensional fault-bend related roll-overs and hanging-wall syncline structures produced during Tortonian to Messinian extensional collapse of the Tell FTB, coeval to the development of Tortonian to Messinian basins (Booth-Rea et al., 2018; 2020; Gaidi et al., 2020). Meanwhile, shortening at the time propagated further South, in the Tunisian Atlas (Bouaziz et al., 2002; Saïd, Baby, Chardon et al., 2011, Saïd, Chardon, Baby et al., 2011). Extensional continental semigrabens in Northern Tunisia have been dated as Early Tortonian (11.6-10 Ma) in the Nefza mining district area using mammalian biostratigraphy and U-Th/He dating of supergene iron oxide mineralizations (Yans et al., 2021).

Tectonic inversion in Northern Tunisia occurred since the Pliocene-Quaternary, marked by a prominent angular unconformity in reflection seismic lines, developing new basin depocenters over the footwall of reverse faults and oblique strike-slip faults (e.g. Melki et al., 2010; 2011; Ayed-Khaled et al., 2015; Gaidi et al., 2020; Camafort et al., 2020a). Many of the reverse fault segments formed by tectonic inversion of earlier Late Miocene normal faults, especially those bounding sedimentary depocenters, such as the Mejerda and Mateur sedimentary basins (Booth-Rea et al., 2018; Gaidi et al., 2020). The main fault system accommodating this late Pliocene to Present-day convergence across Northern Tunisia is the Alia-Thibar dextral reverse fault zone (Gaidi et al., 2020).

3 Methods

For analyzing the structure of Northern Tunisia, together with the metamorphism undergone by the Triassic rocks of Northern Tunisia, we use a multidisciplinary approach. We carried out field work with structural geology emphasis, and also to sample different Triassic evaporite bodies in the region. Our work is based on 1:50.000 geological maps of Northern Tunisia published by the Office National des Mines (ONM), which we digitized and revised (Booth-Rea et al., 2018; Gaidi et al., 2020). Furthermore, we interpreted several industry multichannel reflection seismic lines from the Tunisian Company of Petroleum Activities (ETAP) that cross through the Mejerda basin in Northwestern Tunisia. Triassic pelitic samples from different massifs in Northern Tunisia we analyzed using X-ray diffraction techniques to determine their illite crystallinity. SEM microscopy, RAMAN spectra and electron microprobe were used to analyze the mineral paragenesis in metapelites and metadolerites from the Tell thrust stack. Chlorite-wKm-biotite mineral parageneses were tested for local equilibria using mineral compositions and TWQ thermobarometry software (Berman, 1991). Finally, we used LA-ICP-MS measurements for the radiometric U-Pb dating of metamorphic rutile in the metabasites. Further, methodological details are exposed in the Supporting Information S1.

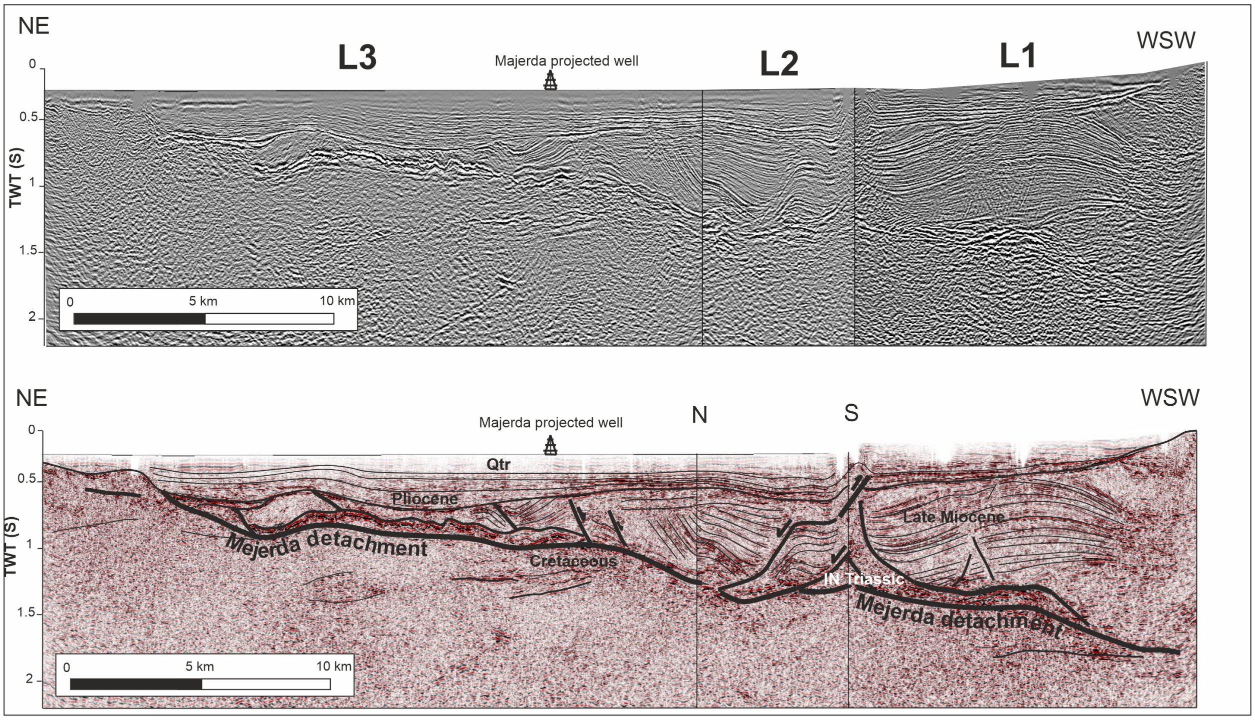

Figure 3: seismic cross-section composition using multichannel reflection seismic lines L1, L2 and L3 through the Mejerda basin, showing normal fault listric fan cutting through Late Miocene sediments and rooting in the Mejerda detachment. Notice low-angle footwall ramp cutting through Cretaceous sediments cut in the Majerda well. The hanging-wall structure is pierced by several halokinetic structures rooted in the Infranumidian Triassic.

4 Structure of Northern Tunisia

4.1 Extensional detachments and halokinetic structures in reflection seismics

Seismic lines across the Mejerda basin show a prominent reflection cutting down southwards at a low angle into the Atlas Cretaceous autochthonous sediments (Seismic lines Mejerda 1, 2, 3 and 4, Figures 2, 3 and 4). This reflector has been cored in the Mejerda 1 drill hole and it separates Triassic evaporites above from underlying Middle Cretaceous marly limestones (Troudi et al., 2017, Figure 2). Meanwhile, the Triassic is overlain by a discontinuous and incomplete section of Mesozoic sediments, mostly Eocene limestones (Troudi et al., 2017). This Mesozoic basement sequence is covered by Middle-Late Miocene to Quaternary sedimentary infilling of the Mejerda basin. The Middle-Late Miocene sediments are cut by high-angle normal faults detaching into the prominent reflection at the base of the Triassic evaporites, showing progressive angular unconformities and halokinetic intrusions over the evaporitic detachment, hereafter named the Mejerda detachment.

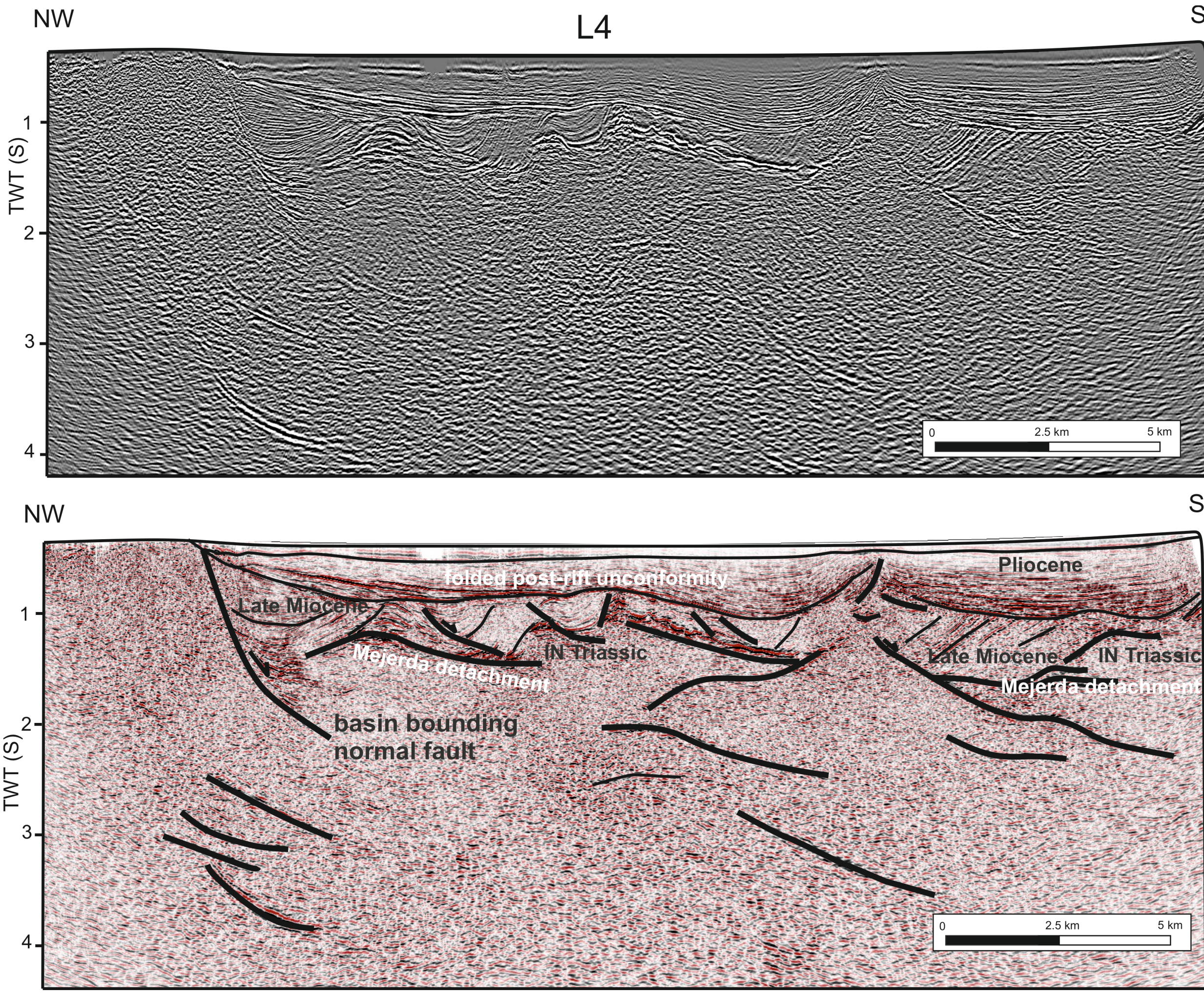

Figure 4: Seismic reflection line L4 across the Mejerda basin, showing high-angle faults exhuming the autochthonous Atlas rocks to the NW and tilted Late Miocene sediments overlying the Mejerda detachment. Late Plio-Quaternary folding is also evident in this line. This seismic line has been published before down to 2sTWT, with different interpretations by Ayed-Khaled et al. (2015); Khelil et al. (2019) and Frifita et al. (2020).

Overall, the Mejerda detachment separates two crustal wedges, an overlying one, thickening towards the South, formed by Infranumidian rocks and overlying Late Miocene sediments, and an underlying one, thinning towards the South formed by Atlas Cretaceous sediments (Figure 3). These extensional structures are overlain by an angular post-rift unconformity, sealed by folded Pliocene to Quaternary sediments. Along lines 1, 2 and 3, the Mejerda detachment deepens towards the SW from 500 to 1800 ms at the SW border of the basin (Figure 3).

Triassic evaporites form boudin type bodies together with high-amplitude packages, interpreted as Eocene limestones, cropping out nearby, above the detachment and below the Late Miocene sediments (Ayed-Khaled et al., 2015). Normal faults overlying the Mejerda detachment show listric geometry, with both SW- and NE-directed kinematics (Figure 3). Overall, the normal faults cutting the Late Miocene sediments form a listric fan structure that roots into the

Mejerda detachment. Few reflectors dipping smoothly towards the NE occur in the footwall of the Mejerda detachment, indicating a low-angle ramp geometry below the detachment.

The extensional structures are overlain by an angular post-rift unconformity, sealed by folded Pliocene to Quaternary sediments. Along lines 1, 2 and 3, the Mejerda detachment deepens towards the SW from 500 to 1800 ms at the SW border of the basin (Figure 3). Triassic evaporites form boudin type bodies together with high-amplitude packages, interpreted as Eocene limestones, cropping out nearby, above the detachment and below the Late Miocene sediments (Ayed-Khaled et al., 2015). Normal faults overlying the Mejerda detachment show listric geometry, with both SW- and NE-directed kinematics (Figure 3). The normal faults cutting the Late Miocene sediments form a listric fan structure that roots into the Mejerda detachment. Few reflectors dipping smoothly towards the NE occur in the footwall of the Mejerda detachment, indicating a low-angle ramp geometry below the detachment.

4.2 Structure derived from field outcrops

Epizonal rocks occur in the Hairech, Ichkeul and Oued Belif massifs in Northern Tunisia (Cross-sections in Figure 2). These rocks are marbles and metapsamnites formed by the metamorphism of Jurassic limestone and underlying Triassic red-beds, dolostone, limestone with intercalated dolerites. The Hairech massif shows an open antiformal WSW-ENE trending structure with its northern and southern limbs cut by high-angle normal faults with NW and SE directed transport, respectively (Rouvier, 1977; Khelil et al., 2019; Khomsi, Roure and Verges, 2022)(cross-section, Figure 2). These normal faults bound the Messinian sediments of the Mejerda basin, both to the North and South of the massif, and also, cut mineralized outcrops of Eocene allochthonous Infra-Numidian rocks (cross section A-A´, Figure 2).

Triassic rocks bearing a low-angle cataclastic foliation crop out along both the Northern and Southern margins of the Mejerda basin (Figure 5a). These rocks crop out extensively in the region forming the base of the hanging-wall of the Mejerda detachment, for example, to the E-SE of Fernana, and also in the region around Thibar (Figure 2). These Triassic rocks, are directly overlain by extensional riders of diverse rocks like the Numidian Flysch, Eocene limestones or Cretaceous-Palaeogene Infra-Numidian sediments, and also by tilted Late Miocene sediments (see geological map and cross section A-A´, Figure 2).

The Mejerda detachment crops out to the South of the Mejerda basin, uplifted in the hanging wall of the Pliocene to Quaternary thrust that deforms the southern margin of the basin (Gaidi et al., 2020, Figure 2). The detachment fault zone is formed by a foliated cataclastic breccia affecting different Triassic lithologies, including red beds, dolostone and gypsum (Figure 5a). This Triassic sequence that crops out largely along the Thibar anticline is itself detached over autochthonous Early Cretaceous marls (Mcherga Formation) that form the core of the anticlinal structure (see Geological map in Figure 2). These features coincided with those observed in the seismic lines crossing the Mejerda basin (Figures 3 and 4). To the East of Fernana, the Mejerda detachment shows a low-angle footwall ramp, cutting down towards the South from Eocene to Turonian-Santonian sediments (cross section A-A´, Figure 2).

High-angle normal faults cutting into the Numidian Flysch sequence define semigrabens filled by Late Miocene conglomerates in the Kroumerie massif (Figure 2 and 5b). These faults exhume the Mejerda detachment at their footwall, exposing Triassic evaporites and overlying Infra-Numidian tectonic units, below the Numidian Flysch. Furthermore, they define the main valleys within the Kroumerie massif. We show the prolongation of these faults towards the SW in section A-A′ in Figure 2.

Figure 5: Field outcrop photographs and related fault and mylonitic foliation data. a) Foliated breccia affecting Triassic rocks in the Mejerda detachment. Notice cataclastic foliation and rotated porphyroclasts in the fault zone. b) Ichkeul marbles showing NW-SE oriented stretching lineation (L1) and mylonitic (Sm) foliation, later cut by calcite veins. c) Thin section of a greenshist metapelitic sample from the Ichkeul dome, notice Sm and S0 folitations and growth of large chlorite crystals parallel to the Sm fabric. d) Thin section showing a metapelitic band marked by white mica growth intercalated in calcite marble. e) Normal fault cutting through the southern limb of the Ichkeul dome, with SE-directed extension. f) Thin section of a metapsamnite from the Hairech dome, showing large white mica crystals defining a metamorphic foliation in these rocks. g) Panoramic view of the Tell-Atlas contact near Balta. Notice the missing infranumidian Eocene limestones, cut by a normal fault, along the supposed thrust contact between the Numidian Flysch and the underlying autochthonous series. Laterally, towards the West, this contact also has Triassic evaporites, which are also ommitted in this section. We relate the missing series along this contact to extensional reworking of the original thrust contact by the activity of the Mejerda detachment.

The Mejerda detachment and overlying Triassic rocks have been folded and thrusted over the whole sedimentary sequence of the Mejerda basin along its southern border during the Plio-Quaternary (Gaidi et al., 2020). This tectonic inversion also affected the Northern margin of the basin, along the Balta-Fernana thrust, a process the uplifted the Mejerda detachment in the hanging wall of the thrust, forming the southern contact of the Kroumerie Numidian Flysch outcrops and the Kasseb unit, over the autochthonous Atlas Cretaceous (Fig. 5c). The Kasseb unit includes Eocene limestones that form prominent discontinuous extensional horses detached over the Mejerda detachment (landscape photo in Figure 5c). We interpret an equivalent structure along section A-A´, partly exposed in the Rebiaa massif (cross-section A-A´, Figure 2).

The Chemtou marbles, and underlying Triassic metapsamnites crop out in an anticlinal structure along the northwestern border of the Mejerda basin. This antiformal structure produces a prominent WSW-ENE oriented ridge with a positive gravimetric anomaly all along the border of the basin, coinciding with the Hairech and Rebiaa massifs (Amiri et al., 2011; Frifita et al., 2020)(See cross-section A-A´ in Figure 2). These massifs are bounded by WSW-ENE trending normal faults that separate the metapsamnites and marbles in their core from strongly mineralized Eocene carbonates and Messinian sediments to the Northwest. Meanwhile, the southeastern border of the massifs also coincides with an WSW-ENE trending high-angle normal fault imaged in seismic line L4 (Figure 4). This normal fault cuts through the whole structure described above rooting in low-angle reflectors at a depth of approximately 3 s TWT (Fig. 4). Marbles and metapsamnites from the Hairech massif show a penetrative foliation, marked by the growth of white mica and chlorite parallel to the lithological banding. However, we did not observe an associated stretching lineation. These rocks do contain a magnetic fabric, related to a strong preferred crystallographic orientation in phyllosilicates, interpreted as a probable syn-metamorphic stretching lineation, with WNW-ESE to WSW-ENE orientation (Ghorabi and Henry, 1992).

Outcrops of Triassic metapelites in the Oued Belif dome are strongly overprinted by mineralizations and magmatic related processes (Decrée et al., 2014, 2013; Mahdi et al., 2013). These metamorphic rocks contrast with the overlying Paleogene and Eocene Infra-Numidian sediments, marking a pronounced metamorphic gap between epizonal and diagenetic rocks (cross section B-B´, Figure 2). Exhumation related structures in this region are particularly clear and intimately related to magmatic processes, with a well-defined brittle-ductile shear zone between the Triassic metapelites and overlying sediments, namely, the Nefza detachment (Booth-Rea et al., 2018). The main extensional detachment produced Eastwards directed extension during the extrusion of rhyodacites that show a magmatic foliation that is parallel to an overlying mylonitic foliation in marbles from the footwall of the Nefza detachment. These rocks are cut by a Late Miocene strongly mineralized fault breccia (Booth-Rea et al., 2018). This exhumation trend, with ductile structures evolving towards brittle breccias is also followed by magmatism in the region that evolves from plutonic intrusion of granodiorites in the Serravallian (12 Ma) to the shallower extrusion of volcanic rocks in the Tortonian (8-9 Ma)(Halloul and Gourgaud, 2012; Decree et al., 2014).

Metamorphic marbles and calcschists crop out in the Ichkeul massif in Northeastern Tunisia affecting Jurassic and late Triassic protoliths (cross section B-B´, Figure 2). This massif occurs isolated by Quaternary sedimentary infilling to the North of the Mateur basin (Figure 2). The marbles are presently folded in the core of an anticline with a WSW-ENE oriented axis. The southern limb of the anticline is cut by two sets of E-W and N-S trending high and low-angle normal faults with mostly S-SE and E-NE directed transport, respectively (Figures 5d and e, with faults and striae projected in stereoplot). Marbles in the Ichkeul massif show a marked blastomylonitic foliation, containing a SW-NE stretching lineation, which in turn is cut by a penetrative system of NW-SE trending calcite veins (Figure 5f, including stereoplot of foliation and lineation). At microscopic scale, biotite and chlorite growth define the mylonitic foliation (S_m) that cuts the older compositional banding (S_0) defined by pelite-carbonate layers (Fig. 5g).

		10Å		5Å			d_{001}	
Samples	**Minerals**	<2μ*	WF	<2μ	WF	b mica	mica	chlorite
CHemtou-1	quartz, mica, Kfds, hematite, smectite↑, kaolinite	0.26	0.26	0.26	0.26	9.032	9.978	
CHemtou-2	quartz, mica, plagioclase, hematite	0.30	0.28	0.28	0.27	9.038	9.971	
MT-1	mica, Kfds, quartz↓, jarosite	0.27	0.27	0.25	0.26			
ICH-04	calcite↑, kaolinite, mica, Kfds	0.29	0.26	0.30	0.25			
ICH-05	quartz, calcite, mica↓, plagioclase, smectite							
MT-2	quartz, mica, dolomite, cristobalite	0.32	0.32	0.32	0.29			
MT-3	quartz, mica, dolomite, cristobalite, Kfds↓	0.34	0.31	0.32	0.28			
MT-4	quartz, mica, smectite, Kaolinite, dolomite↑	0.31	0.32	0.32	0.28			
MT-5	quartz, mica, chlorite, gypsum	0.57	0.46	0.56	0.43			
CH1	quartz, mica, chlorite, hematite↓,Kfds↓↓	0.47	0.46	0.41	0.38	9.029	9.971	14.19
FB-01	dolomite↑, mica, chlorite, quartz↓	0.37	0.37	0.35				14.19
TA-01	quartz, mica, chlorite, Kfds, plagioclase	0.42	0.42	0.39	0.36	9.024 9.044	9.945	14.21
	↑, ↓, ↓↓ = qualitative indication of amount							
	*Anchizone limits (Warr and Ferreiro Mählmann, 2015) =		0.52	-	0.32			
	WF - Whole Fraction							

Table 1: Illite crystallinity results and mineralogy of Triassic pelitic samples. Samples located in the geological map of Figure 2.

5 Metamorphic petrology

5.1 Illite crystallinity

X-Ray diffraction results indicates quartz, white mica ± K-feldspar ± plagioclase ± hematite ± dolomite ± calcite (Table 1). Some of the samples from the Infra-Numidian Triassic also contain chlorite or cristobalite and one sample gypsum. Moreover, minerals usually linked to low-temperature alteration processes, like smectite, kaolinite or jarosite exist in the samples in very variable proportions.

Illite crystallinity (KI) of the Triassic metapelites cropping out in the Tunisian Tell shows two different populations (Table 1, see location in Figure 2). Samples (Chemtou01, Chemtou02, MT-1, ICH-04) picked from the deep autochthonous Triassic outcrops from Oued Belif, Hairech and Ichkeul anticlinal domes are characterized by typical epizonal values between 0.26 and 0.30 (Table 1). Meanwhile, the allochthonous Triassic located at the base of the Infra-Numidian nappe is characterized by a range between diagenetic values (0.57, MT-5) and mostly anchizonal values between 0.33 and 0.47 (MT-2, MT-3, CH1, FB-01 and TA-01), together with an epizonal value in sample MT-4.

The number of mica b parameters in the metamorphic autochthonous Triassic outcrops is between 9.032 and 9.038 Å, which would be characteristic of orogenic micas grown under an intermediate P/T metamorphic gradient (Guidotti and Sassi, 1986). Basal spacing of chlorites in the allochthonous Triassic is considerably high (14.19-14.20), which indicates high Si content (Nieto, 1997), which, in turn, suggests low temperature chlorites (Vidal et al., 2016 and references therein).

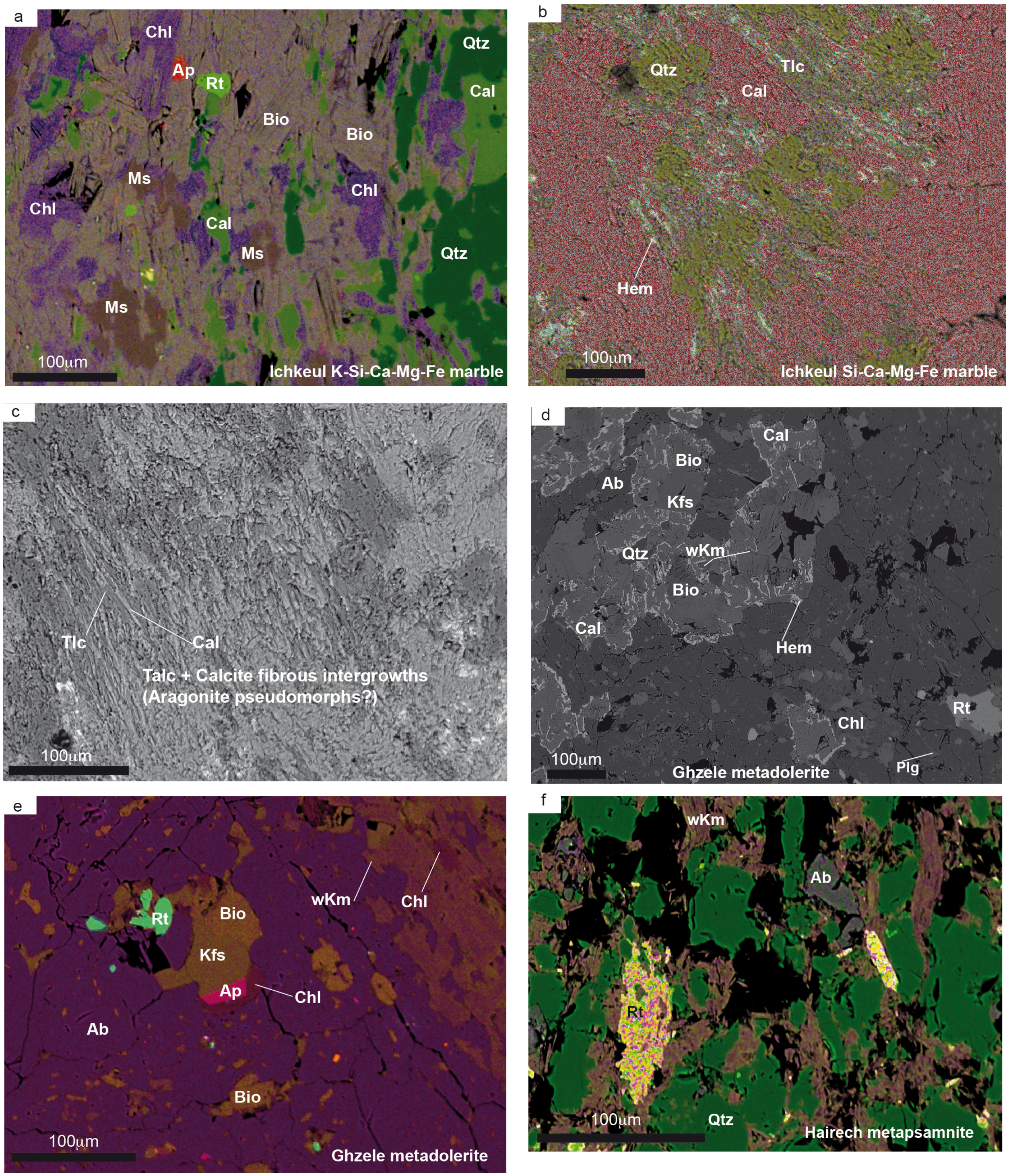

437 **Figure 6:** Mineral paragenesis and textures from the Tunisian epizonal domes. a) Mineral association in Ichkeul K-Si-Ca-Mg-Fe calcschist bands. b) Calcite+quartz+talc+hematite mineral association growing in Ichkeul Si-Ca-Mg-Fe marbles. c) Detail of Talc+quartz+calcite fibrous intergrowths, which probably represent aragonite pseudomorphs. d) Mineral association in Ghzele-b metadolerite formed by biotite + Kfeldspar + quartz + calcite + albite + chlorite + rutile + hematite + white K mica + Na-Ca plagioclase. e) Detail of rutile and apatite growing in the Ghzele-b

metadolerite. f) Metapsamnite of the Hairech massif with detrital quartz grains with white K mica beards. The mineral association also includes albite and rutile.

5.2. Metamorphic mineral assemblages in metadolerites, metapelites and calcschist

Psammitic and impure marble samples from the Hairech and Ichkeul domes, representing the structurally deepest rocks in Northern Tunisia show lower-greenschist mineral paragenesis defined by chlorite + white K mica + albite + epidote. Meanwhile, the samples from Ichkeul show a mylonitic foliation and compositional banding defined by white K mica + chlorite + biotite + calcite + quartz in Si-Al-Mg-Fe-K-Ca marbles overprinting an earlier metamorphic fabric defined by a talc + calcite + quartz assemblage in Si-Mg-Fe-Ca marbles (Figure 6a and b). Talc shows fibrous intergrowths with quartz and calcite, which has an habitus similar to aragonite or aragonite pseudomorphs described elsewhere (Brady et al., 2004; Chopin et al., 2008; Gerogiannis et al., 2021)(Figure 6c). Meanwhile, calcschist in Ichkeul show two generations of mica, an older one formed by white K mica and a more recent biotite growing in pressure shadows around phengite and chlorite (Figure 6a).

Metadolerite blocks occur within the Ghzele detachment at the base of the Infranumidian Triassic sequence at intermediate depths within the Tunisian Tell FTB. These rocks also occur at other Triassic outcrops in Northern Tunisia, near Bazina and in Jebel Baoula, overlying the Atlas Cretaceous autochthonous rocks (Kurtz, 1983) (Cross-section B-B′, Figure 2). Moreover, they are described further south in the Le Kef diapir (Kurtz, 1983). We have studied two metadolerite samples from the Ghzele detachment (Ghzele-a and -b) that show variable degrees of metamorphic and metasomatic alteration as described by Kurtz (1983) in all metadolerite outcrops of Northern Tunisia. Metadolerite Ghzele-a is strongly overprinted by a metamorphic paragenesis defined by albite+chlorite+epidote+calcite+quartz. The original magmatic assemblage is only represented by relic plagioclase and titanomagnetite crystals. Metadolerite Ghzele-b shows a further transformation where K-rich minerals replace the metamorphic assemblage described in Ghzele-a. These include potassium-feldspar, white K mica and a Mg-rich biotite. Moreover, the later sample is rich in calcite, hematite, apatite and rutile (Figure 6d and e). A metapsamnite of the Hairech massif shows white K mica+quartz+albite+rutile, with mica beards growing around quartz detrital grains (Figure 6f).

5.3. Mineral chemistry

We determined the mineral assemblage and analyzed the composition of different minerals within metabasites, metapsamnites and calcschists from both the deeper metamorphic domes and from metabasites at intermediate depths in the Tell nappe stack, using multiple tools including electron microprobe, SEM and RAMAN spectra analysis. The compositions of wKm, biotite and chlorite were determined using a Camebax electron microprobe from the Granada University. Structural formulae were calculated based on 14 (anhydrous) oxygens for chlorite and 11 for micas.

5.3.1. White K mica

White K micas show variable amounts of Si and interlayer cation content both within individual rock samples and between epizonal rock massifs. This variability manifests changing metamorphic pressure and temperature, leading to different proportions of mica compositional end members, represented by muscovite, celadonite, pyrophyllite and paragonite. Si content responds to exchanges among the muscovite, celadonite and pyrophyllite end members. Tchermak ($2Al_{IV}=Si_{IV}+(Fe+Mg_{VI})$) substitution between the celadonite and muscovite end members is strongly influenced by pressure (Massonne and Schreyer, 1987; Massonne and Szpurka, 1991), whilst Si enrichment, together with interlayer cation deficiency between the muscovite and pyrophyllite end member ($K_{XII}\text{-}1Al_{IV}\text{-}1Si_{IV}\square_{XII}$) is sensitive to a decrease of temperature (Agard et al., 2001; Leoni et al., 1998; Vidal and Parra, 2000)

1997). WKm from the Ichkeul Massif show Si contents between 3.26 and 3.0 a.p.u.f. and interlayer cation content (IC) between 0.81 and 0.98 a.p.u.f., marking a trend towards lower Si content and higher interlayer occupancy that would indicate a heating during decompression metamorphic P-T path (Table S2 and Figure 7a). WKm from the Hairech Massif show strongly variable compositions with Si contents ranging between 3.52 and 3.12 a.p.u.f. and IC between 0.83 and 0.98 a.p.u.f., which suggest strong pyrophyllitic substitution characteristic of low-temperature micas and probably also relatively high P/T metamorphic gradient (Figure 7b).

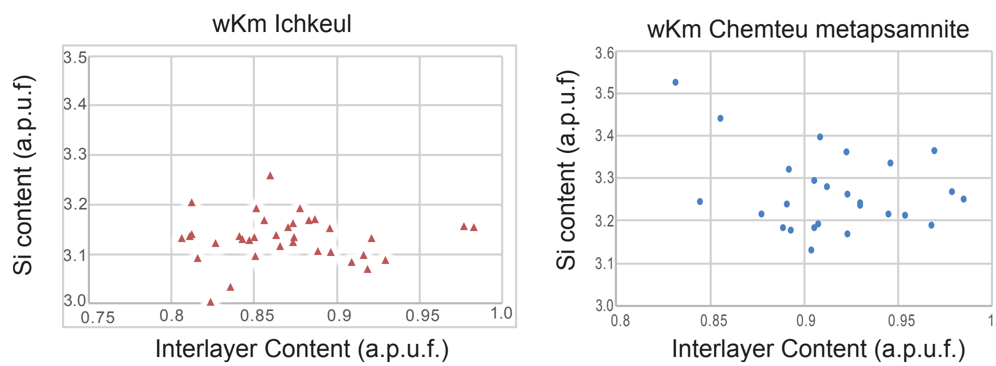

Figure 7: Si-Interlayer cation content of white K micas of Northern Tunisia. a) white K micas from the Ichkeul dome. b) white K micas from metapsamnites underlying the Chemteu marbles, from the Hairech massif. Notice composition variability indicating their crystallization under a wide range of P-T conditions.

5.3.2. Chlorite

Chlorite analysis in the Ichkeul blastomylonitic calcschists give Si contents ranging between 2.94 and 2.65 a.p.u.f., XMg between 0.50 and 0.64 and octahedral summation between 5.77 and 5.90 a.p.u.f. (Table S3). Compositional variability between the different chlorite compositional end members, including clinochlore, daphnite, amesite and sudoite depends on the metamorphic conditions as well as the rock chemistry (Jenkins and Chernosky, 1986; Vidal and Parra, 2000; Vidal et al. 2005).

Fe^{3+} content in chlorite cannot be determined using the electron microprobe, however, its value is important for thermobarometric calculations in the KFMAS system. We estimate Fe^{3+} in chlorite by minimizing the differences between P-T conditions resulting from two different equilibrium calculations using thermodynamic properties published by Vidal et al. (2005). The first only involves chlorite end members (Daphnite, Clinochlore, Fe-Amesite and Mg-Amesite). Since only three of these four end members are independent, this equilibrium must be satisfied to obtain the same solid-solution free energy calculated with either clinochlore, daphnite, Fe-, or

Mg-amesite (Vidal et al., 2005). The second equilibrium involves Qtz and H_2O, within the KMAS system (Clin+Sud=Mg-Am+Qtz+H2O). We obtain values of XFe3+ between 0.3 and 0.41, below maximum values actually measured in Chlorite (Lanari et al., 2014; Trincal et al., 2015). Chlorite in the Ghzele metadolerite shows high Si contents ranging between 2.96 and 3.00 a.p.u.f., XMg from 0.72 to 0.73 and octahedral summation between 5.90 and 5.99 a.p.u.f., which may correspond to low temperature chlorites (Table S3).

5.3.3. Biotite

Biotite in the Ichkeul calcschists shows variable compositions with Si content between 2.77 and 2.89 a.p.u.f., XMg from 0.56 to 0.61 (Table S4). It is the most abundant mineral in the pelitic intercalations of the Ichkeul marbles and grows replacing chlorite and white K mica.

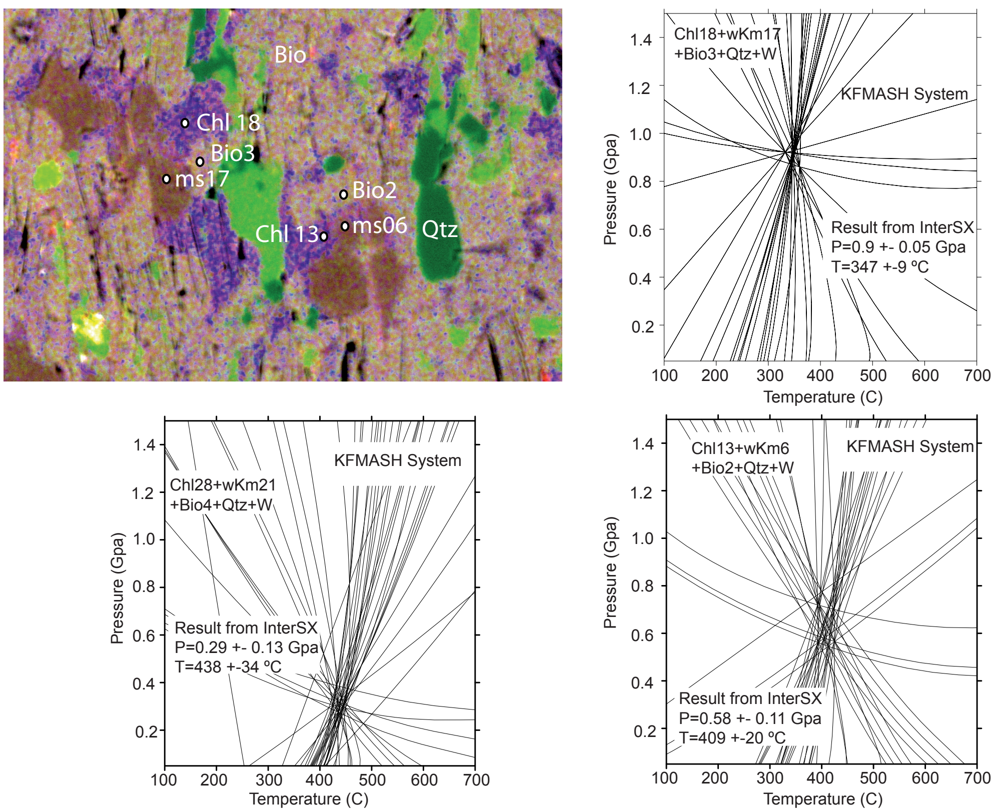

Figure 8: Analyzed mineral assemblages from the Ichkeul calcshist and resulting TWQ thermobarometric results indicating HP/LT metamorphism, followed by heating and decompression during the growth of blastomylonitic foliation.

5.4. Multiequilibrium P-T results

We obtained preliminary multiequilibrium P-T data for chlorite + white K mica + biotite + quartz + water assemblage defining the main foliation in the Ichkeul calcschist. Multiequilibrium results were calculated using TWQ 1.02 software (Berman, 1991) and its associated database JUN92, updated with more recent thermodynamic properties and solid solution models for chlorite and white K mica (Parra et al., 2002 and Vidal et al., 1992, 1999, 2005). Fe 3+ in chlorite was obtained as described in the chlorite mineral chemistry section, above. Calculations were done assuming a water activity of 1.0, which, may be unprecise, although, the presence of talc in these rocks implies high water activity (e.g. Bucher and Grapes, 2011).

Obtained P-T equilibria, with four independent reactions, show that the Ichkeul rocks reached HP-LT conditions of 0.9 ± 0.05 Gpa at 347 ± 9 ºC during the growth of phengite-rich white K micas (Si=3.26 a.p.u.f.), within the stability field of aragonite + talc in intercalated Mg-Si-Fe marbles (Figure 8). Later chlorite, biotite and white K mica growth developed during decreasing pressure at higher temperature with equilibria, for example, at 0.58 ± 0.11 Gpa at 409 ± 20 ºC and at 0.29 ± 0.13 at 438 ± 34 ºC (Figure 8). These later conditions would correspond to blastomylonitic deformation under NE-SW stretching in the Ichkeul marbles (Figure 5f, g).

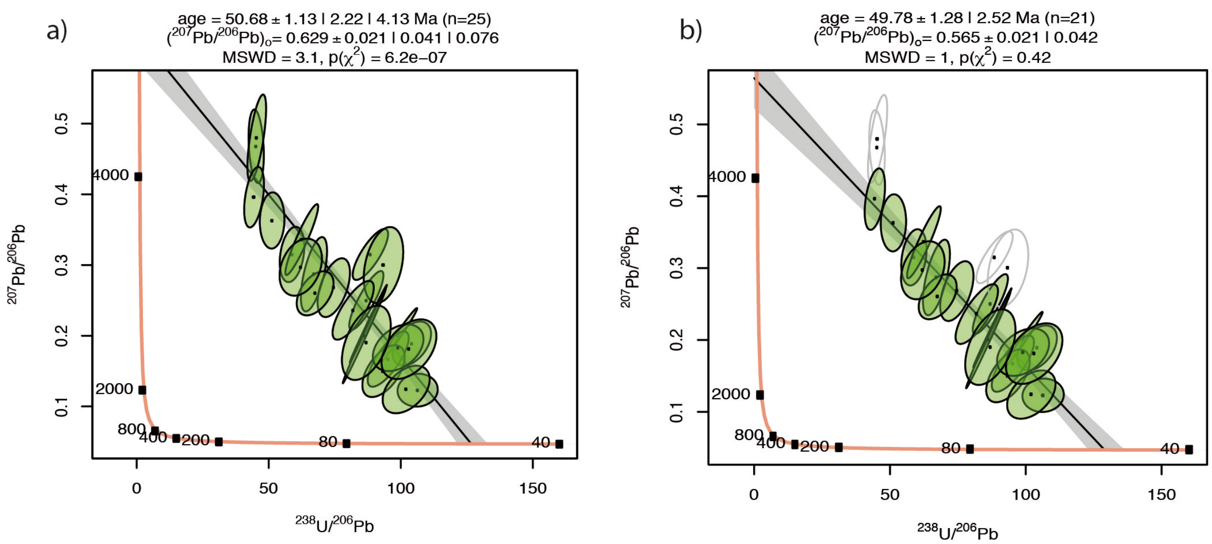

Figure 9: Tera-Wasserburg diagrams of rutile. Discordia isochron ages were calculated with IsoplotR (Vermeesch, 2018) using the least-square "York" method without anchored common $^{207}Pb/^{206}Pb$. Error ellipses in Tera-Wasserburg diagrams are displayed with 95%-confidence level. a) Results with all analysis. b) Results excluding selected analysis shown as grey ellipses.

5.5. Rutile U-Pb LA-ICP-MS dating

Rutile crystals were analyzed by LA-ICP-MS in sample Ghzele-b (Figure 6 d and e) and data shown in Figure 9 and provided in Table S5. Rutile U-Pb are sufficiently radiogenic to be analyzed and yield a Tera–Wasserburg Discordia date of 50.68 ± 1.13 Ma (2σ, n = 25, MSWD = 13.1) (Figure 9 a) considering all the analyses, and of 49.78 ± 1.28 Ma (2σ, n = 21, MSWD = 1.0; ($^{207}Pb/^{206}Pb)_o$= 0.56 ± 0.02) (Figure 9 b), excluding selected analyses (shown as grey ellipses). These analyses likely reflect an event date between c. 51 and 48 Ma.

6 Discussion

6.1. Low-temperature metamorphism in the Tunisian Tell

The new illite crystallinity data and metamorphic assemblages we show in this study together with previous data in the region (Mahdi et al., 2013) manifests the presence of lower-greenschist epizonal rocks in the core of the structurally deepest domal Triassic outcrops of Northern Tunisia (Table 1, cross-sections and samples in Figure 2). These Permo-Triassic rocks have been interpreted as forming the outcropping base of the autochthonous Mesozoic Atlassic sedimentary cover, deposited in the North Maghrebian passive margin (Rouvier, 1993, 1992; Booth-Rea et al., 2018). The fact that these minerals show clear metamorphic textures and illite crystallinity values below the limit between anchizone and epizone imply they underwent temperatures above 300 ºC characteristic of mid-crustal depths (Frey, 1987; Merriman and Roberts, 1985; Merriman and Peacor, 1998).

Some samples contain variable proportions of smectite, kaolinite and jarosite, which are low-temperature minerals, incompatible with the metamorphic conditions described for the Triassic outcrops. The occurrence of these low-temperature minerals in rocks of higher diagenetic-metamorphic grades has been often described and interpreted as the result of retrograde diagenesis (Abad et al., 2003; Nieto et al., 2005), fluid-mediated retrograde processes occurring under diagenetic conditions. In particular, do Campo et al., (2017) linked the existence of jarosite in anchizonal/epizonal rocks of the Central Andes with the activity of hydrothermal fluids producing acid type alteration, related with the posthumous activity of the Ordovician volcanic arc; this alteration produced the widespread occurrence of retrograde diagenesis products as smectite and kaolinite in slates and metavolcanic rocks. Similar volcanic activity occurred in Northern Tunisia, especially obvious in the Oued Belif dome, which together with the hydrothermal activity related to extensional faulting can easily explain the presence of these retrograde mineral phases in the studied samples.

The scattering of KI values for the Infranumidian Triassic that crops out in a large area all along Northern Tunisia may represent original depth differences within the Tell orogenic wedge. The diagenetic value in sample MT-5 is located to the SE, theoretically, close to the Tell deformation front, where the Triassic is directly covered by Early Miocene fore-deep olistostromic sediments at the Lansarine ridge (Figure 2). Meanwhile, most of the samples further towards the W or NW give anchizonal values, reflecting an original deeper position within the orogenic wedge. Sample MT-4 with epizone values is located at the footwall of the Ghzala extensional detachment a few meters below the fault zone, in the Jalta Pb-Zn mine, coexisting with the studied metadolerites, which underwent clear greenschist facies metamorphism (Figure 6d).

The illite crystallinity data are further supported by the mineral associations we found in the Ichkeul calcschist and marbles including biotite + wKm + chlorite + quartz + calcite (Figure 6a) and calcite + dolomite + talc + chlorite + hematite (Figure 6b), respectively, which would require temperatures between 300 ºC and 470 ºC, in the stability of talc and biotite and below the stability of tremolite (Bucher and Grapes, 2011). Furthermore, our multiequilibrium thermobarometric results for the deepest outcrops of the Tunisian Tell, corresponding to the Ichkeul marbles confirm these conditions and indicate that these rocks underwent HP-LT metamorphism under blueschist facies at approximately 0.9-1.0 Gpa and 350 ºC, followed by decompression and heating to conditions of 0.6-0.3 Gpa and 400-440ºC during the growth of biotite (Figure 8). Decompression during heating is also manifested by the compositional trend in white K mica, showing decrease in Si content together with an increase in interlayer cation content (Figure 7). The HP-LT conditions we obtained fall within the stability of talc and aragonite in impure Mg-Si-Fe marbles (Bucher and Grapes, 2011). This may indicate that elongated calcite fiber intergrowths with talc and quartz could represent aragonite pseudomorphs in the Ichkeul marbles (Figure 6c).

The infranumidian Triassic rocks cropping out above the Ghzela and Mejerda extensional detachments, below the Numidian nappes, reached anchizonal to diagenetic conditions below 300ºC. Although, the growth of biotite, K-feldspar and rutile in metadolerites included in these rocks, together with the nearby epizonal sample MT-04, suggest even higher temperatures above 300 ºC. Meanwhile, towards the SE of the Tell orogenic wedge at the tip of the deformation front the Triassic rocks underwent lower temperatures not surpassing diagenetic conditions. At present, the whole nappe stack, between epizonal rocks at the base and diagenetic Numidian series at the top has a total thickness around 3 s TWT (Booth-Rea et al., 2018) that would correspond to around 4 km depth using a velocity of 2.7 km/s for the sediments of the Tell belt.

The HP/LT thermobarometric results in the Ichkeul marbles indicate that the epizonal Atlas Triassic domes reached a typical orogenic P-T gradient of approximately 15 ºC/km during a HP-LT metamorphic event and were exhumed from under approximately 25 km overburden provided by the Tell nappe stack. This evolution parallels the one observed in the Betics and external Rif (e.g. Azañón et al., 1998; Booth-Rea et al., 2002; Negro et al., 2007). This assertion is supported by the present structure of the Tell belt that shows extensional listric fans overlying low-angle normal faults at least at two different structural levels, corresponding to the Ghzela and Mejerda detachments, and the deeper Nefza detachment that flattens around 3s TWT (Booth-Rea et al., 2018).

The Ghzela and Mejerda detachments produced ENE-WSW directed extension cutting down into the Tell orogenic wedge and reaching anchizonal depths, whilst the Nefza detachment reached mid-crustal depths of approximately 15-10 km, under temperatures of 400-440 ºC where deformation was governed by dynamic recrystalization creep during the growth of biotite, producing the mylonitic foliation and SW-NE stretching lineation observed in the Ichkeul massif marbles (stereoplot and photo in Figure 5f). Alternatively, the blastomilonitic foliation in the Ichkeul massif may have formed by shearing under shortening conditions during the Late Burdigalian (17 Ma) as described for similar structures in the Temsamane massif in the Eastern Rif (Jabaloy et al., 2015).

6.2. From Cretaceous extensional to Eocene and Early Miocene orogenic metamorphism in Northern Tunisia

Integrating our new rutile U-Pb 49.78 ± 1.28 Ma results with previously published radiometric dating indicates a polymetamorphic evolution for the Tunisian Tell, similar to the one observed at the opposite end of the Maghrebian Alpine chain, in the Rif (Vazquez et al., 2013; Jabaloy et al., 2015). K-feldspar and phlogopite K-Ar ages from metadolerites and marbles from different outcrops in the Tunisian Tell give Cretaceous (97 ± 5 to 67 ± 3 Ma), Palaeocene (65 ± 3), Oligocene (27 ± 1 to 25 ± 1) and Miocene ages (23 ± 1,2 to 17,6 ± 0,9) (Bellon and Perthuisot, 1977). Although, this age dispersion was interpreted as a result of Cretaceous extensional-sedimentary load related metamorphism, mixed with radiometric resetting by late

Neogene magmatic heating in the region (Bellon and Perthuisot, 1977), we provide a new alternative scenario.

Most of these ages probably represent distinct metamorphic events, related to different geodynamic stages in the evolution of the Western Mediterranean. Late Cretaceous ages between 97 and 69 Ma may correspond to very-low grade spilitic metamorphism probably produced by the sedimentary-related overburden in the North-Maghrebian passive margin, described in the Tellian metadolerites (Kurtz, 1983). Equivalent ages and metamorphic conditions were obtained for anchizonal rocks of the Ketama unit in the external Rif (Vázquez et al., 2013; Jabaloy et al., 2015). The new rutile U-Pb 49.78 ± 1.28 Ma data we present, together with the Latemost Cretaceous to Paleocene ages reported by Bellon and Perthuisot (1977), must represent initial stages of plate convergence between Africa and Eurasia, evidencing tectonic inversion and crustal thickening at the transition between the North Maghrebian passive margin and the Tethys ocean, at the time. This crustal thickening and related deformation favored the mineral blastesis in the Tellian metadolerites producing the K-feldspar, biotite and rutile paragenesis. Between the Cretaceous and Eocene, subduction was active in the Alps (Rubatto et al., 1998; Villa et al., 2014; Malusà et al. 2015). This metamorphism coincides with shortening along the Atlas in the Latemost Cretaceous-Eocene (de Lamotte et al., 2009).

The studied metadolerites presently crop out among anchizonal to epizonal Triassic evaporites at the base of the Infra-Numidian nappe stack , overlying lower-grade autochthonous Atlas Cretaceous sediments of the Atlas series, which reached conditions between inmature and early to mid-mature oil generation according to Rock-Eval pyrolysis testing (Ben Ammar et al., 2020), implying temperatures probably below 150 ºC (e.g. Buller et al., 2005). Thus, this Early Eocene crustal thickening-related metamorphism occurred before the establishment of the present Tellian nappe stack, in a transitional region between the Tethyan oceanic crust and the Maghrebian passive margin.

The main phase of nappe stacking in the Tunisian Tell is dated as Early Miocene by the overthrusting of the Oligocene to Burdigalian Numidian flysch sandstones over Late Burdigalian to Langhian sediments of the Glauconite formation (Belayouni et al., 2013). However, the Tell accretionary wedge and NE directed subduction of the Tethys ocean initiated earlier as attested by both UHP metamorphic mineral growth during the Early Oligocene in the Kabilies (32.4 ± 3.3 Ma, Brougier et al., 2017) and Eocene to Early Oligocene volcanic arc zircons within the Tethyian Flysch units (33 ± 1 Ma, Fornelli et al., 2020 and 40-28 Ma in the Rif, Abbassi et al., 2021). Phlogopite in the Ichkeul marbles at the base of the Tunisian Tell FTB has given 23 ± 1,2 and 17,6 ± 0,9 Ma ages (Bellon and Perthuisot, 1977), and probably grew during the main phase of nappe stack development, as deduced from the new thermobarometric results we obtained with biotite + wKm + chlorite growth in the intercalated calcschists at both HP/LT and later IP/LT conditions (Figure 8). Actually, the growth of biotite during heating, decompression and ductile stretching suggests that the younger ages may reflect the initial extensional collapse of the Tunisian Tell, which had already occurred in the internal Kabilies in Argelia, marked by late-stage K-rich magmatism intruding the nappe stack, dated at 17 Ma (Abbassene et al., 2016; Chazot et al., 2017).

6.3. Halokinetic structures in Northern Tunisia

We find two main types of Triassic outcrops, the shallower of which, develop halokinetic structures related mostly to the late Neogene extensional phase, and the deeper ones are represented by exhumed middle crust formed by autochthonous Triassic redbeds and marbles. The first type of Triassic bodies outcrop extensively in the Thibar, Lansarine or Bazina regions and have traditionally been interpreted as salt canopies or glaciers overlying the Atlas Cretaceous series (e.g. Masrouhi et al., 2014; Ayed-Khaled et al., 2015; Amri et al., 2020). However, these sheet-like bodies are not only overlain by Cretaceous sediments, but also by tilted extensional riders of Eocene limestones and Late Miocene sediments, for example in Ghzela, at the Jalta mine, and Mateur basin (Booth-Rea et al., 2018), Lansarine ridge (Gaidi et al., 2020, Figure 10) or in the Mejerda basin (Seismic lines and cross section A-A´, Figures 2 and 3). Moreover, the fact that the Triassic evaporites underwent Early Eocene epizonal metamorphism as demonstrated by the growth of U-Pb dated rutile, Kfeldspar and biotite, which is not present in the underlying Cretaceous sediments, means they juxtaposed these rocks during a later thrusting stage.

We interpret that the shallower anchizonal to diagenetic infra-Numidian evaporites and redbeds were originally emplaced at the base of the Numidian and Infra-numidian nappes and were later reworked by the Mejerda and Ghzela extensional detachments and related normal faults, developing shallow depth halokinetic structures rooting in the extensional LANFs. These evaporitic outcrops form salt walls along the main high-angle normal faults, define the main extensional detachments, and also form small diapiric bodies rooting in the LANFs (Figures 3 and 4). Moreover, these structures have been re-used and inverted during the later Plio-Quaternary shortening in the region (Gaidi et al., 2020).

The deeper Triassic bodies are found in antiformal dome-type outcrops, where epizonal and HP/LT orogenic crust has been exhumed from midcrustal depths in the Oued Belif, Ichkeul and Hairech massifs (cross sections A-A´ and B-B´, Figure 2). These metamorphic domes were produced by ductile flow and extensional exhumation of the North Tunisian orogenic middle crust during the Middle to Late Miocene and do not represent diapirs.

6.4. Extensional exhumation in Northern Tunisia

Our field and geophysical evidence shows different systems of extensional faults that detach at two different structural positions within the Tell nappe stack (Booth-Rea et al., 2018). The shallower LANFs, represented by the Ghzela and Mejerda detachments that show NE and SW-directed extension, cut down into the Mesozoic Atlas sequence producing the Mateur and Mejerda basin depocenters. These faults exhume mostly the Eocene to Cretaceous Atlas sequence. The younger extensional structures produce mostly SE-directed extension and are formed by a system of high-angle listric faults that cut the above detachments and root at depths of approximately 3s TWT. These faults bound the Hairech (cross section A-A´, Figure 2) and Ichkeul massifs (Figures 5 d, e) and outcrop along the Lansarine massif, where the Infranumidian Triassic and overlying Early to Late Miocene sediments are tilted over a low-angle normal fault with SE-transport cutting down into Cretaceous Atlas sediments (Gaidi et al., 2020, Figure 10).

The extensional systems worked sequentially, the first system produced mostly eastwards to northeastard directed extension during the Tortonian (≈11-8 Ma), and maybe including the Serravallian, with the development of brittle LANFs like the Mejerda, Ghzele and brittle-ductile shear zones like the Nefza detachment. The NE-SW directed ductile stretching observed in the Ichkeul dome may have initiated earlier during the Langhian coinciding with the younger phlogopite K-Ar ages obtained in this massif (Bellon and Perthuisot, 1977). However, the final exhumation of these midcrustal rocks to the surface was accomplished by a later orthogonal extensional system, producing mostly southwards directed extension during the Tortonian to Messinian ((≈8-5) Ma. High-angle normal faults, cutting LANFs of this later system are the structures that presently bound the Hairech and Ichkeul mid-crustal domes in Northern Tunisia (Figures 4, 5e, cross sections in Figure 2).

Figure 10: Example of two orthogonal extensional systems cutting Late Miocene sediments and thinning the Early Miocene Tell FTB nappe pile along the Lansarine ridge in Northern Tunisia. Notice Tortonian extensional rider tilted over a normal fault with SE-directed transport, overlying Atlas Cretaceous marls tilted towards the NW. The SE-directed extension affects the older Mejerda extensional detachment, where Infranumidian Triassic evaporites overlie Cretaceous autochthonous sediments. The Mejerda detachment thins and reworks the previous Early Miocene nappe contact between the Infranumidian and Atlas domains.

This work shows that the main tectonic boundaries present in the Tunisian Tell were strongly reworked during the late Miocene extensional collapse of Northern Tunisia. The remains of the original Late Oligocene to Early Miocene nappe pile that formed the Tell orogenic belt are now cut and displaced by low-angle normal faults and extensional detachments that exhumed the Tunisian orogenic middle crust, producing important tectonic omissions and metamorphic gaps in the lithological sequences, during the Late Miocene (cross section A-A´, Figures 2, 5 c). The late Miocene extension in Northern Tunisia propagated Southeastwards during the Pliocene to Quaternary, affecting large regions of Central Tunisia, the Sicilian

Channel and the Pelagian domain offshore (Civile et al., 2010; Belguith et al., 2011; 2013; Arab et al., 2020)(Figure 10). This extension probably followed earlier Middle Miocene extension towards the NE and concomitant openning of the Easternmost segment of the oceanic Algerian basin (Haidar et al., 2022 ; Figure 11).

6.5. Extensional tectonics and related geodynamic features of Tunisia

This tectonic model for Tunisia explains many geophysical characteristics of the region that are not explained by a model of protracted, only shortening, since the Cretaceous and has to be taken into consideration when restoring and defining the main orogenic belts in Northern Tunisia. Our work shows that allochthonous anchizonal Triassic rocks we have attributed to the Infra-Numidian domain crop out to the South of the classical Tell boundary, indicating that the Tell orogenic wedge originally occupied a larger region towards the South than presently considered. Actually, the boundaries established for this orogenic belt coincide with the Present position of active shortening structures that formed since the Pliocene, like the Alia-Thibar fault system (Gaidi et al., 2020), which produces the main seismicity in the area (Soumaya et al., 2015) and accommodates most of the GPS measured shortening of the region (Bougrine et al., 2019).

Heat flow in Tunisia shows present-day values around 80-90 mW/m^2 with higher values towards the E of Tunisia (Lucazeau and Dhia, 1989). This heat flow is higher than observed in typical active FTB´s around the world (Morgan and James, 1989; Booth-Rea et Al, 2008; Lucazeau, 2019). Furthermore, lithospheric thickness shows a strong decrease from values above 180 km South of the Tunisian South Atlassic thrust and values around 140 (Globig et al., 2016) and probably less under the Southern Atlas STEP boundary where negative shear wave velocity anomalies are observed around 80-100 km depth (Radi et al., 2017). This relative thin lithospheric thickness in Tunisia is also accompanied by abundant hydrotermalism in the region (Dhia, 1987) and related high-temperature Fe-Zn-Pb mineralizations (>190 ºC) produced since the Late Miocene (e.g. Benchilla et al., 2003; Decrée et al., 2008; Jemmali et al., 2014; Aïssa et al., 2018), data that suggests even higher heat flow values in the Tortonian for the whole region. Several geophysical studies support the existence of a mantle slab underlying central Tunisia (Research group for lithospheric structure in Tunisia, 1992 ;Jallouli and Mickus, 2000; Piromallo and Morelli, 2003; Faccenna et al., 2014; Fichtner et al., 2015; El-Sharkawy et al., 2020.)(Figure 10).

Extension in Northern Tunisia has been related to the E to SE retreat and peeling-back of the slab body described above, under Tunisia since the Late Miocene, which would include a strip of Nubian continental lithospheric mantle (Roure et al., 2012; Booth-Rea et al., 2018; Camafort et al., 2020). The older extensional system migrated eastwards, towards the direction of slab retreat, and was thus, probably related to delamination of the lithospheric mantle inboard of the South Tunisian Atlas STEP boundary (Figure 10). Meanwhile, the later southwards directed extension was accompanied by important topographic uplift that migrated towards the E-SE in the late Miocene (Salah and Vanhouten, 1988), reaching the eastern coast of Tunisia in the Quaternary. This extension and the related topographic uplift we propose may be associated with flexural and isostatic rebound after the delamination under Northern and probably Central Tunisia (Roure et al., 2012 ; Booth-Rea et al., 2018). This tectonic mechanism drove active extension, magmatism, hydrothermalism and topographic uplift in the region, processes that migrated behind the retreating slab. Slab retreat was favored by slab tearing or detachment at the edge of the system along the Southern Tunisian Atlas thrust front that has been interpreted as a dextral STEP boundary that continues active at Present day (Booth-Rea et al., 2018; Camafort et al., 2020; Soumaya et al., 2020)(TA-STEP, Figure 11).

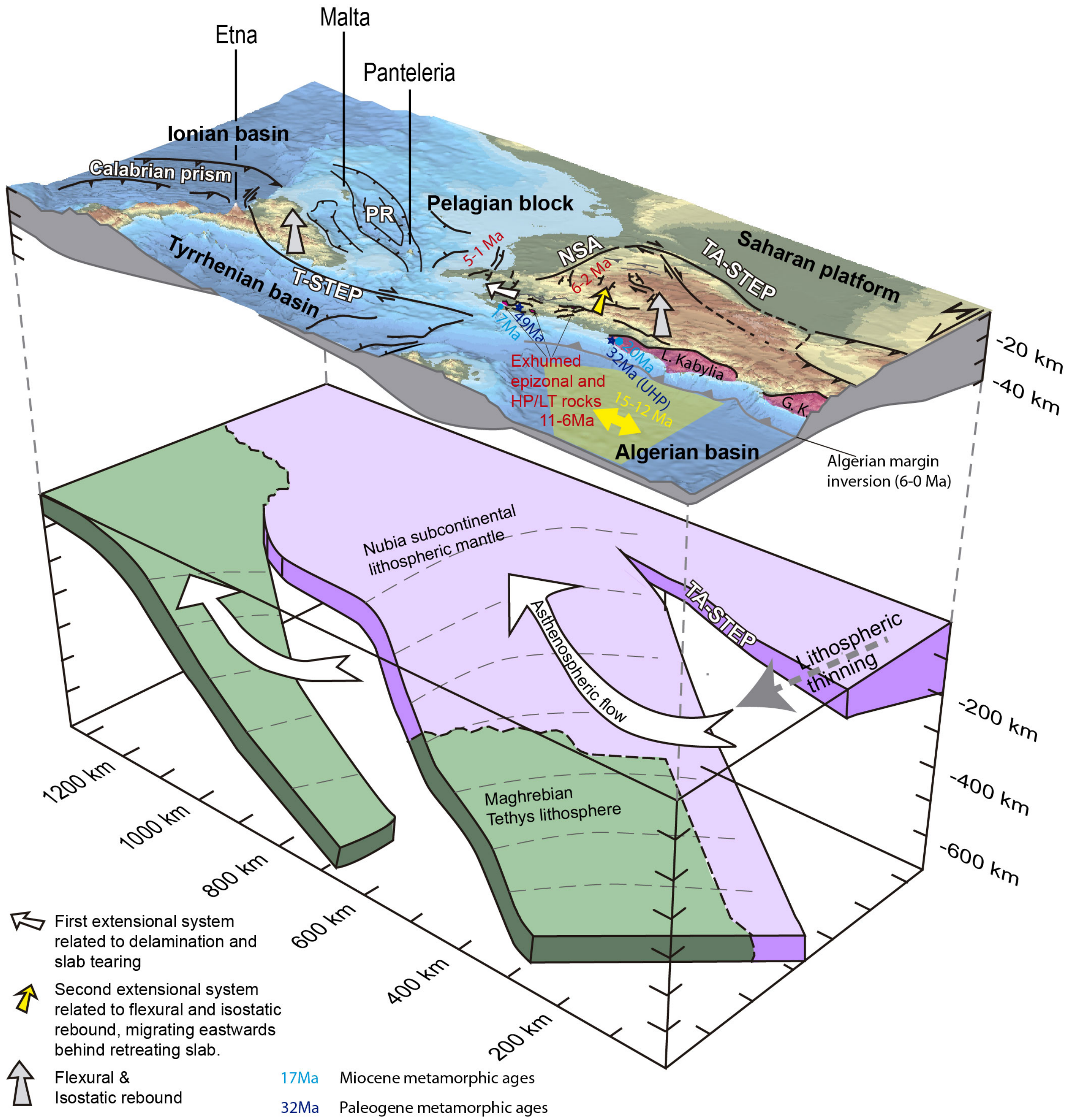

Figure 11: Cartoon of the tectonic mechanisms driving mid-crustal exhumation in Northern Tunisia and the location of exhumed middle crust in the region. Notice the thinning of the Tunisian-Algerian lithosphere across the Tunisian Atlas STEP boundary (TA-STEP). NE-SW extension initiated in the Middle Miocene coeval to the oppening of the East Algerian Basin (Haidar et al., 2022) and propagated into Northern Tunisia in the Tortonian (approx. 11-8 Ma), meanwhile, later SE-directed extension finally exhumed the Tunisian metamorphic domes, including the Ichkeul

HP/LT blastomylonites, in the Late Tortonian-Messinian (approx. 8-5.3 Ma). Exhumed metamorphic rocks include Early Eocene metadolerites (Rutile U-Pb 49.78 ± 1.28 Ma) and Early Miocene (23 and 17 Ma phlogopite K-Ar, Bellon and Perthuisot, 1977) HP/LT blastomylonitic marbles and calcschist in the easternmost Ichkeul dome. Figure background, modified from Booth-Rea et al. (2018).

6.6. FTB extension in the Western Mediterranean

The structure of the Tell in Northern Tunisia resembles strongly the one observed in other external FTB´s of the Western Mediterranean, like the External Rif domain in Morocco, where epizonal orogenic crust was exhumed in the Temsamane massif during the Tortonian (Negro et al, 2007; Booth-Rea, 2012; Figure 1). The Betics FTB also has metamorphic rocks that underwent pumpellyite-actinolite facies metamorphism under approximately 300ºC and 4-5 kbar (Puga et al., 1988; Morata et al., 1994), which were probably exhumed through extensional tectonics (Azañón et al., 2012; Rodríguez-Fernández et al., 2011; 2013). At the same time, deeper HP/LT rocks from the subducted Iberian passive margin were exhumed from mid-crustal depths, under the allochthonous hinterland rocks, by ductile-brittle detachments in the Betics (e.g. Jabaloy et al., 1993; Martínez-Martínez and Azañón, 1997; Martínez-Martínez et al., 2002; Booth-Rea et al., 2005; 2015; Morales et al., 2022). In all cases, the extensional structures affect the external FTB structure developed during the Early to Late Miocene in the Rif, Betics and Tell orogenic belts (Figure 1). Extension propagated behind the FTB development, exhuming rocks from mid-crustal depths of the previously established accretionary wedge (Booth-Rea et al., 2012, 2020).

Abridging, the structure observed in Northern Tunisia is comparable to other FTB´s in the Western Mediterranean that were extended between the Middle Miocene and Recent (e.g. Carmignani and Kligfiel, 1990; Ghisetti and Vezzani, 2002; Booth-Rea, 2012; Rodríguez-Fernández et al., 2013; Moragues et al., 2018; 2021, Figure 1). Although, several works suggest that extension in these FTB´s is minor and related to the internal dynamics of the accretionary wedge, for example, to changes in the basal friction related to the presence of underlying evaporites (Jiménez-Bonilla et al., 2016; Khelil et al., 2018), in Northern Tunisia, the Eastern Betics and Eastern Rif extension has resulted in a marked thinning of the crust under the FTB domain and exhumation of metamorphic rocks (Negro et al., 2007; Booth-Rea et al., 2012; 2018; 2020; Azdimousa et al., 2019). In these later cases, where the crust shows thickness below 30 km (Research Group for Lithospheric Structure in Tunisia, 1992; Mancilla et al., 2015; Mancilla and Diaz, 2015) we suggest extension was related to the propagation of the edge of the subduction system under the FTB domain. Thus, the same tectonic mechanisms corresponding to slab tearing and subcontinental lithospheric delamination determined the extensional collapse of FTB´s all around the Western Mediterranean in the Betics, Rif, Tell and Tunisian Atlas, mostly during the late Miocene, and more recently under the Central Apennines (Figure 1).

Heating during decompression coeval to the development of late-stage mylonitic shear zones is a common feature observed in the exhumed metapelites of the South Iberian subducted passive margin (Booth-Rea et al., 2015) and in Northern Tunisia and may be a diagnostic feature of lithospheric mantle delamination and subsequent heating at the base of the crust, together with other associated magmatic processes like K-Si-rich shoshonitic volcanism (Duggen et al., 2003; Booth-Rea et al., 2007; 2018).

Future work should further analyze the age and P-T conditions reached during the metamorphism of the Northern Tunisia extensional domes and the actual extent of the low-angle detachments described here, further South in the Atlas orogenic belt. Furthermore, deep geophysical soundings are necessary to understand the lithospheric structure of Tunisia and the existence or not of an attached lithospheric mantle slab under the region.

7 Conclusions

We present the first U-Pb ion-probe dating of Early Eocene metamorphism related to Africa-Eurasia plate convergence along the North Maghrebian passive margin, producing the blastesis of rutile at 49.78 ± 1.28 Ma.

These new radiometric ages together with previously published K-Ar ages on K-feldspar and phlogopite from metadolerites and marbles in Northern Tunisia indicate the region underwent a polymetamorphic evolution with distinct metamorphic events including Late Cretaceous extensional-spilitic metamorphism, followed by Eocene and Early Miocene metamorphic events related to tectonic shortening along the Tunisian Tell and Atlas.

Our data support alternative tectonic processes to diapirism and protracted shortening since the Cretaceous in Northern Tunisia, corresponding to Late Miocene crustal extension of a previously overthickened orogenic wedge. Our new thermobarometric and metamorphic data, together with illite crystallinity shows that most of the Triassic outcrops in Northern Tunisia are made up by very low-grade and low-grade metamorphic rocks that underwent epizonal or anchizonal conditions.

The Ichkeul dome hosts HP/LT metamorphic rocks with aragonite pseudomorphs and Si-rich phengite equilibrated at 0.9-1.0 Gpa under 350 ºC that were exhumed through heating and decompression to 400-440 ºC at 0.6-0.3 GPa.

We distinguish two different types of Triassic outcrops, corresponding to overthrusted sheet type bodies intercalated in the remains of the extended Tellian thrust stack, which underwent mostly anchizonal to epizonal metamorphism during the Cretaceous to Early Eocene before overthrusting the underlying Atlas sequence, and domal type bodies where the deeper autochthonous Atlas Triassic crops out metamorphosed under HP-LT or epizonal conditions in the Early Miocene. These second, rooted outcrops show evidence of NE-SW directed ductile shearing under temperatures of 400-440 ºC in the footwall of extensional detachments.

Seismic reflection lines in the Mejerda basin show a conspicuous reflector reworking the Infra-Numidian Triassic that corresponds to the Mejerda detachment. The footwall shows a low-angle ramp geometry cutting down southwards into the autochthonous Atlas Cretaceous sediments. This extensional system is cut by later normal faults that root at depths of 3 s TWT that finally exhume the folded Triassic epizonal Ichkeul, Hairech and Oued Belif metamorphic domes.

Most halokinetic structures in Northern Tunisia are rooted in the Mejerda detachment and intruded the overlying sedimentary overburden during the Late Miocene extension. These include salt walls extruding through normal faults and small-scale diapirs. The evaporites have played an important role as decollement surfaces both during late Miocene extension and the later Plio-Quaternary shortening.

The mid-crustal exhumation observed in Northern Tunisia is analogous to the one described in other FTB´s of the western Mediterranean like the Betics and Rif, where delamination and tearing of the lithospheric mantle propagated under the continental FTB domains. Extension of the Western Mediterranean orogenic arcs propagated into the external foreland domains of the Gibraltar, Calabrian and Algerian-Tunisian arcs. Extension was polyphasic, with two orthogonal systems. The older system extended towards the direction of slab retreat under continental FTB domains. Meanwhile, the later system, producing extension transverse to the direction of slab retreat was related to isostatic and flexural rebound that trailed behind the retreating slabs.

Acknowledgments

This study was supported by research projects financed by the Ministerio de Ciencia e innovación PID2019-107138RB-I00 and P18-RT- 3632 of the Junta de Andalucia, Erasmus Mundus External Cooperation Window and by Scientific Cooperation Agreement 0534 between the Office National des Mines (ONM), the Tunis el Manar University and the Group for Relief and Active Processes Analysis (ARPA) from the University of Granada. We are grateful to the Tunisian Company of Petroleum Activities (ETAP) for sharing their Reflection Seismic Data.

Data Availability Statement

Compositional analyses of different minerals are available as tables in Supplementary Information. Seismic lines and maps used in this manuscript will be archived in a Fishare repository after acceptance.

References

Abad, I., Nieto, F., Peacor, D.R., Velilla, N. (2003). Prograde and retrograde diagenetic and metamorphic evolution in metapelitic rocks of Sierra Espuna (Spain). *Clay Minerals, 38*, 1–23.

Abbassene, F., Chazot, G., Bellon, H., Bruguier, O., Ouabadi, A., Maury, R. C., Déverchére, J., Bosch, D. & Monie, P. (2016), A 17 Ma onset for the post-collisional K-rich calc-alkaline magmatism in the Maghrebides: Evidence from Bougaroun (northeastern Algeria) and geodynamic implications. *Tectonophysics, 674*, 114-134.

Abbassi, A., Cipollari, P., Fellin, M. G., Zaghloul, M. N., Guillong, M., El Mourabet, M., & Cosentino, D. (2021), The Numidian sand event in the Burdigalian foreland basin system of the Rif, Morocco, in a source-to-sink perspective. *GSA Bulletin*. https://doi.org/10.1130/B36136.1

Agard, P., Vidal, O., Goffé, B. (2001), Interlayer and Si content of phengite in HP-LT carpholite-bearing metapelites. *Journal of Metamorphic Geology, 19*, 477–493.

Agostinetti, N. P., Levin, V., & Park, J. (2008), Crustal structure above a retreating trench: Receiver function study of the northern Apennines orogen. *Earth and Planetary Science Letters, 275*(3-4), 211-220.

Aïdi, C., Beslier, M.O., Yelles-Chaouche, A.K., Klingelhoefer, F., Bracene, R., Galve, A., Bounif, A., Schenini, L., Hamai, L., Schnurle, P., Djellit, H., Sage, F., Charvis, P., Déverchère, J. (2018), Deep structure of the continental margin and basin off Greater Kabylia, Algeria – New insights from wide-angle seismic data modeling and multichannel seismic interpretation. *Tectonophysics 728*–729, 1–22. https://doi.org/10.1016/j.tecto.2018.01.007

Axelsson, E., Pape, J., Berndt, J., Corfu, F., Mezger, K.and M. M. Raith (2018), Rutile R632 – A New Natural Reference Material for U-Pb and Zr Determination, *Geostandards and Geoanalytical Research, 42*(3), 319-338, doi:doi:10.1111/ggr.12213.

Azdimousa, A., Jabaloy-Sánchez, A., Münch, P., Martínez-Martínez, J. M., Booth-Rea, G., Vázquez-Vílchez, M., Asebriy, L., Bourgois, J. & González-Lodeiro, F. (2019), Structure and exhumation of the Cap des Trois Fourches basement rocks (Eastern Rif, Morocco). *Journal of African Earth Sciences, 150*, 657-672.

Amiri, A., Chaqui, A., Nasr, I.H., Inoubli, M.H., Ayed, N. Ben, Tlig, S., 2011. Role of preexisting faults in the geodynamic evolution of Northern Tunisia, insights from gravity data from the Medjerda valley. *Tectonophysics, 506*, 1–10.

Amri, Z., Naji, C., Masrouhi, A., & Bellier, O. (2020), Interconnection salt diapir–allochthonous salt sheet in northern Tunisia: the Lansarine–Baoula case study. *Journal of African Earth Sciences, 170*, 103876. https://doi.org/10.1016/j.jafrearsci.2020.103876

Arab, M., Maherssi, C., Granjeon, D., Roure, F., Déverchère, J., Cuilhé, L., Hassaim, M., Mouchot, N., Doublet, S., Khomsi, S. (2020). On the origin and consequences of crustal-scale extension between Africa and Sicily since Late Miocene: insights from the Kaboudia area, western Pelagian Sea. *Tectonophysics, 795*, 228565..

Ayed-Khaled, A., Zouaghi, T., Atawa, M., & Ghanmi, M. (2015), New evidence on the geologic setting of Medjerda Valley plain (northern Tunisia) from integrated geophysical study of Triassic evaporite bodies. *Annals of geophysics, 58*(3), S0326. https://doi.org/10.4401/ag-6567

Ayed-Khaled, A., Ghanmi, M., & Zargouni, F. (2012), Filtering of the gravimetric anomalies to the study of the geological structures of Oued Zarga (Septentrional Tunisia): structural implications. *Arabian Journal of Geosciences, 5*(1), 169-180.

Azañón, J.M., García-Dueñas, V., Goffe, B. (1998), Exhumation of High-Pressure Metapelites and Coeval Crustal Extension in the Alpujarride Complex (Betic Cordillera). *Tectonophysics, 285*, 231-252.

Azañón, J.M., Roldán, F.J., Rodríguez Fernández, J. (2012), Fallas y despegues extensionales en el Subbético Central: implicaciones en la evolución Neógena de las Zonas Externas de La Cordillera Bética. *Geogaceta, 52*, 107-110.

Babist, J., Handy, M. R., Konrad-Schmolke, M., & Hammerschmidt, K. (2006), Precollisional, multistage exhumation of subducted continental crust: The Sesia Zone, western Alps. *Tectonics, 25*(6).

Bedir, M., Boukadi, N., Ben Timzal, F., Zitouni, L., Alouani, R., Slimane, F., Bobier, C., Zargouni, F., Bédir, M., Ben Timzalreceived, F. (2001), Subsurface Mesozoic basins in the central Atlas of Tunisia: tectonics, sequence deposit distribution, and hydrocarbon potential. *AAPG bulletin, 85*(5), 885-907. https://doi.org/10.1306/8626CA2D-173B-11D7-8645000102C1865D

Belayouni, H., Guerrera, F., Martín-Martín, M., Serrano, F. (2013), Paleogeographic and geodynamic Miocene evolution of the Tunisian Tell (Numidian and Post-Numidian Successions): bearing with the Maghrebian Chain. *International Journal of Earth Science, 102*, 831-855.

Belayouni, H., Brunelli, D., Clocchiatti, R., Staso, A. Di, Hassani, I.E.E.A. El, Guerrera, F., Kassaa, S., Ouazaa, N.L., Martin, M.M., Serrano, F., Tramontana, M. (2010), La Galite Archipelago (Tunisia, North Africa): Stratigraphic and petrographic revision and insights for geodynamic evolution of the Maghrebian Chain. *Journal of African Earth Science, 56*, 15–28. https://doi.org/10.1016/j.jafrearsci.2009.05.004

Belguith, Y., Geoffroy, L., Mourgues, R., Rigane, A. (2013), Analogue modelling of Late Miocene – Early Quaternary continental crustal extension in the Tunisia – Sicily Channel area Tunisia. *Tectonophysics, 608*, 576–585. https://doi.org/10.1016/j.tecto.2013.08.023

Belguith, Y., Geoffroy, L., Rigane, A., Gourmelen, C., Ben, H. (2011), Neogene extensional deformation and related stress regimes in central Tunisia. *Tectonophysics, 509*, 198–207.

https://doi.org/10.1016/j.tecto.2011.06.009

Bellon, H., & Perthuisot, V. (1977), Ages radiometriques (K/Ar) de feldspaths potassiques et de micas neoformes dans le Trias de Tunisie septentrionale. *Bulletin de la Société Géologique de France*, *7*(5), 1179-1184.

Ben Aïssa, L., Alouani, R., & Ben Aïssa, W. (2018), Tectono-magmatic events and genesis of Fe-Pb-Zn resources in Nefza area, NW Tunisia. *Arabian Journal of Geosciences*, *11*(20), 1-14.

Ben Ammar, S., Riahi, S., Belhadj Mohamed, A., & Layeb, M. (2020), Source rock characterization of the upper Barremian, Albian and Cenomanian–Turonian organic-rich strata outcropping in Oued Bazina area, NE of Thibar diapir: Northern Tunisia. *Arabian Journal of Geosciences, 13*(24), 1-21.

Benaouali-Mebarek, N., de Lamotte, D. F., Roca, E., Bracene, R., Faure, J. L., Sassi, W., & Roure, F. (2006), Post-Cretaceous kinematics of the Atlas and Tell systems in central Algeria: Early foreland folding and subduction-related deformation. *Comptes Rendus Geoscience, 338*(1-2), 115-125.

Ben Chelbi, M., Melki, F., Zargouni, F. (2006), Mode of salt bodies emplacement in Septentrional Atlas of Tunisia. Example of a Bir Afou salt body. *Comptes Rendus - Geoscience, 338*, 349–358. https://doi.org/10.1016/j.crte.2006.02.009

Benassi, R., Jallouli, C., Hammami, M., Turki, M.M. (2006), The structure of Jebel El Mourra, Tunisia: a diapiric structure causing a positive gravity anomaly. *Terra Nova, 18*, 432–439.

Benchilla, L., Guilhaumou, N., Mougin, P., Jaswal, T., Roure, F. (2003), Reconstruction of palaeo-burial history and pore fluid pressure in foothill areas: a sensitivity test in the Hammam Zriba (Tunisia) and Koh-i-Maran (Pakistan) ore deposits. *Geofluids, 3*, 103–123.

Berman, R.G. (1991), Thermobarometry using multi-equilibrium calculations: a new technique, with petrological applications. *Canadian Mineralogist, 29*, 833-855.

Booth-Rea, G., Azañón, J.M., Martínez-Martínez, J.M., Vidal, O., García-Dueñas, V. (2005), Contrasting structural and P-T evolution of tectonic units in the southeastern Betics: Key for understanding the exhumation of the Alboran Domain HP/LT crustal rocks (western Mediterranean). *Tectonics, 24*, 1-23.

Booth-Rea, G., Klaeschen, D., Grevemeyer, I. and Reston, T. (2008), Heterogeneous deformation in the Cascadia convergent margin and its relation to thermal gradient (

Washington , NW USA). *Tectonics, 27*, 1–15. https://doi.org/10.1029/2007TC002209

Booth-Rea, G., Jabaloy-Sánchez, A., Azdimousa, A., Asebriy, L., Vílchez, M. V., & Martínez-Martínez, J. M. (2012), Upper-crustal extension during oblique collision: The Temsamane extensional detachment (eastern Rif, Morocco). *Terra Nova, 24*(6), 505-512. https://doi.org/10.1111/j.1365-3121.2012.01089.x

Booth-Rea, G., Gaidi, S., Melki, F., Marzougui, W., Azañón, J.M., Galvé, J.P., Pérez-Peña, J. V, Ruano, P (2020), Comment on "How to build an extensional basin in a contractional setting? Numerical and physical modelling applied to the Mejerda basin at the front of the eastern tell of Tunisia" by Mannoubi Khelil et al. *Journal of Structural Geology, 138*, 103935. https://doi.org/https://doi.org/10.1016/j.jsg.2019.103935

Booth-Rea, G., Gaidi, S., Melki, F., Marzougui, W., Azañón, J.M., Zargouni, F., Galvé, J.P., Pérez-Peña, J. V. (2018), Late Miocene Extensional Collapse of Northern Tunisia. *Tectonics, 37*, 1626–1647. https://doi.org/10.1029/2017TC004846

Booth-Rea, G., Martínez-Martínez, J.M., Giaconia, F. (2015), Continental subduction, intracrustal shortening, and coeval upper-crustal extension: PT evolution of subducted south Iberian paleomargin metapelites (Betics, SE Spain). *Tectonophysics, 663*, 122–139.

Booth-Rea, G., Ranero, C.R., Martínez-Martínez, J.M., Grevemeyer, I. (2007), Crustal types and Tertiary tectonic evolution of the Alborán sea, western Mediterranean. *Geochemistry, Geophysics and Geosystems, 8*(10). https://doi.org/10.1029/2007GC001639

Bouaziz, S., Barrier, E., Soussi, M., Turki, M.M., Zouari, H. (2002), Tectonic evolution of the northern African margin in Tunisia from paleostress data and sedimentary record. *Tectonophysics, 357*, 227–253. https://doi.org/10.1016/S0040-1951(02)00370-0

Boukaoud, E. H., Godard, G., Chabou, M. C., Bouftouha, Y., & Doukkari, S. (2021), Petrology and geochemistry of the Texenna ophiolites, northeastern Algeria: Implications for the Maghrebian flysch suture zone. *Lithos, 390*, 106019.

Bougrine, A., Yelles-chaouche, A.K., Calais, E. (2019), Active deformation in Algeria from continuous GPS measurements. *Geophysics Journal International, 217*, 572–588. https://doi.org/10.1093/gji/ggz035

Bouillin, J.-P., Durand Delga, M., Olivier, P. (1986), Betic-Rifian and Tyrrhenian Arcs : Distinctive Features, Genesis and Development Stages, in F. Wezel (Ed.), *The Origin of Arcs. Developments in Geotectonics, 21*, 281-304.

https://doi.org/https://doi.org/10.1016/B978-0-444-42688-8.50017-5
Boukhalfa, K., Soussi, M., Ozcan, E., Banerjee, S., Tounekti, A. (2020), The Oligo-Miocene siliciclastic foreland basin deposits of northern Tunisia: Stratigraphy, sedimentology and paleogeography. *Journal of African Earth Science, 170*, 103932.
Bracène, R., & de Lamotte, D. F. (2002), The origin of intraplate deformation in the Atlas system of western and central Algeria: from Jurassic rifting to Cenozoic–Quaternary inversion. *Tectonophysics, 357*(1-4), 207-226.
Bracciali, L., Parrish, R. R., Horstwood, M. S. A., Condon, D. J. and Najman Y. (2013), UPb LA-(MC)-ICP-MS dating of rutile: New reference materials and applications to sedimentary provenance, *Chemical Geology, 347*, 82-101, doi:10.1016/j.chemgeo.2013.03.013.
Brady, J. B., Markley, M. J., Schumacher, J. C., Cheney, J. T., & Bianciardi, G. A. (2004), Aragonite pseudomorphs in high-pressure marbles of Syros, Greece. *Journal of Structural Geology, 26*(1), 3-9.
Brogi, A. (2008), Kinematics and geometry of Miocene low-angle detachments and exhumation of the metamorphic units in the hinterland of the Northern Apennines (Italy). *Journal of Structural Geology, 30*(1), 2-20.
Bruguier, O., Bosch, D., Caby, R., Vitale-Brovarone, A., Fernandez, L., Hammor, D., Laouar, R., Ouabadi, A., Abdallah, N., Mechati, M. (2017), Age of UHP metamorphism in the Western Mediterranean: insight from rutile and minute zircon inclusions in a diamond-bearing garnet megacryst (Edough Massif, NE Algeria). *Earth and Planetary Science Letters, 474*, 215–225.
Bucher, K., & Grapes, R. (2011), Metamorphism of dolomites and limestones. In: *Petrogenesis of metamorphic rocks* (pp. 225-255). Springer, Berlin, Heidelberg.
Bugini, R., Folli, L., Marchisio, R. (2019), "Giallo Antico" in Roman Architecture of Lombardy: A Preliminary Survey, in *Conference of the Arabian Journal of Geosciences. Springer*, 107–109.
Buller, A. T., Bjørkum, P. A., Nadeau, P. H., & Walderhaug, O. (2005), Distribution of hydrocarbons in sedimentary basins. *Research & Technology Memoir, 15*.
Camafort, M., Gràcia, E., & Ranero, C. R. (2020), Quaternary Seismostratigraphy and Tectonosedimentary Evolution of the North Tunisian Continental Margin. *Tectonics, 39*(11), e2020TC006243.

Camafort, M., Pérez-Peña, J. V, Booth-Rea, G., Melki, F., Gràcia, E., Azañón, J.M., Galve, J.P., Marzougui, W., Gaidi, S., Ranero, C.R. (2020), Active tectonics and drainage evolution in the Tunisian Atlas driven by interaction between crustal shortening and mantle dynamics. *Geomorphology, 351*, 106954. https://doi.org/https://doi.org/10.1016/j.geomorph.2019.106954

Carmignani, L., & Kligfield, R. (1990), Crustal extension in the Northern Apennines: the transition from compression to extension in the Alpi Apuane core complex. *Tectonics, 9*(6), 1275-1303.

Carminati, E., Wortel, M.J.R., Spakman, W., Sabadini, R. (1998), The role of slab detachment processes in the opening of the western – central Mediterranean basins : some geological and geophysical evidence. *Earth and Planetary Science letters, 160*, 651–665.

Chazot, G., Abbassene, F., Maury, R. C., Déverchère, J., Bellon, H., Ouabadi, A., & Bosch, D. (2017), An overview on the origin of post-collisional Miocene magmatism in the Kabylies (northern Algeria): evidence for crustal stacking, delamination and slab detachment. *Journal of African Earth Sciences, 125*, 27-41.

Chertova, M. V, Spakman, W., Geenen, T., Van Den Berg, A.P., Van Hinsbergen, D.J.J. (2014), Underpinning tectonic reconstructions of the western Mediterranean region with dynamic slab evolution from 3-D numerical modeling. *Journal of Geophysical Research Solid Earth, 119*, 5876–5902.

Chopin, C., Beyssac, O., Bernard, S., & Malavieille, J. (2008), Aragonite–grossular intergrowths in eclogite-facies marble, Alpine Corsica. *European Journal of Mineralogy, 20*(5), 857-865.

Civile, D., Lodolo, E., Accettella, D., Geletti, R., Ben-Avraham, Z., Deponte, M., Facchin, L., Ramella, R., Romeo, R. (2010), The Pantelleria graben (Sicily Channel, Central Mediterranean): An example of intraplate 'passive' rift. *Tectonophysics, 490*, 173–183. https://doi.org/https://doi.org/10.1016/j.tecto.2010.05.008

Cohen, C.R., Schamel, S., Boyd-Kaygi, P. (1980), Neogene deformation in northern Tunisia: Origin of the eastern Atlas by microplate—continental margin collision. *Geological Society of America Bulletin, 91*, 225–237.

Crespo-Blanc, A., & Campos, J. (2001), Structure and kinematics of the South Iberian paleomargin and its relationship with the Flysch Trough units: extensional tectonics within the Gibraltar Arc fold-and-thrust belt (western Betics). Journal of Structural Geology, 23(10), 1615-1630.

Crespo-Blanc, A., & de Lamotte, D. F. (2006), Structural evolution of the external zones derived from the Flysch trough and the South Iberian and Maghrebian paleomargins around the Gibraltar arc: a comparative study. *Bulletin de la Société géologique de France*, *177*(5), 267-282.

Daudet, M., Mouthereau, F., Brichau, S., Crespo-Blanc, A., Gautheron, C., & Angrand, P. (2020), Tectono-stratigraphic and thermal evolution of the western Betic flysch: implications for the geodynamics of South Iberian margin and Alboran Domain. Tectonics, 39(7), e2020TC006093.

de Lamotte, D. F., Leturmy, P., Missenard, Y., Khomsi, S., Ruiz, G., Saddiqi, O., Guillocheaou, F. & Michard, A. (2009), Mesozoic and Cenozoic vertical movements in the Atlas system (Algeria, Morocco, Tunisia): an overview. Tectonophysics, 475(1), 9-28.

de la Peña, L. G., Ranero, C. R., Gràcia, E., & Booth-Rea, G. (2020), The evolution of the westernmost Mediterranean basins. *Earth-Science Reviews, 214,* 103445.

Decrée, S., Marignac, C., De Putter, T., Deloule, E., Liégeois, J.P., Demaiffe, D. (2008), Pb-Zn mineralization in a Miocene regional extensional context: The case of the Sidi Driss and the Douahria ore deposits (Nefza mining district, northern Tunisia). *Ore Geology Reviews, 34*, 285–303. https://doi.org/10.1016/j.oregeorev.2008.01.002

Decrée, S., Marignac, C., De Putter, T., Yans, J., Clauer, N., Dermech, M., Aloui, K., Baele, J.-M. (2013), The Oued Belif hematite-rich breccia: A Miocene iron oxide Cu-Au-(U-REE) deposit in the Nefza mining district, Tunisia. *Economic Geology, 108*, 1425–1457.

Decrée, S., Marignac, C., Liégeois, J.P., Yans, J., Ben Abdallah, R., Demaiffe, D. (2014), Miocene magmatic evolution in the Nefza district (Northern Tunisia) and its relationship with the genesis of polymetallic mineralizations. *Lithos, 192*, 240-258.. https://doi.org/10.1016/j.lithos.2014.02.001

de Ruig, M. J. (1995), Extensional diapirism in the eastern Prebetic foldbelt, southeastern Spain, in M. P. A. Jackson, D. G. Roberts, and S. Snelson, eds., *Salt tectonics: a global perspective: AAPG Memoir, 65*, 353-367.

Dewey, J.F., Helman, M.L., Knott, S.D., Turco, E., Hutton, D.H.W., Knott, S.D. (1989), Kinematics of the western Mediterranean. *Geological Society London Special Publications, 45*, 265–283. https://doi.org/10.1144/GSL.SP.1989.045.01.15

Dhia, H. B. (1987), The geothermal gradient map of central Tunisia: comparison with structural, gravimetric and petroleum data. *Tectonophysics, 142*(1), 99-109.

Di Luzio, E., Mele, G., Tiberti, M.M., Cavinato, G.P., Parotto, M. (2009), Moho deepening and shallow upper crustal delaminaion beneath the central Apennines. *Earth and Planetary Science letters, 280*, 1–12.

Do Campo, M., Nieto, F., Albanesi, G.L., Ortega, G., Monaldi, C.R. (2017), Outlining the thermal posdepositional evolution of the Ordovician successions of northwestern Argentina by clay mineral analysis, chlorite geothermometry and Kübler index. *Andean Geology, 44*, 179–212. https://doi.org/10.5027/andgeoV44n2-a04

Duggen, S., Hoernle, K., van den Bogaard, P., Rüpke, L., Phipps Morgan, J. (2003), Deep roots of the Messinian salinity crisis. *Nature, 422*, 602–606. https://doi.org/10.1038/nature01553

El Ghali, A., Ayed, N. B., Bobier, C., Zargouni, F., & Krima, A. (2003), Les manifestations tectoniques synsédimentaires associées à la compression éocène en Tunisie: implications paléogéographiques et structurales sur la marge Nord-Africaine. *Comptes Rendus Geoscience, 335*(9), 763-771.

El-Sharkawy, A., Meier, T., Lebedev, S., Behrmann, J. H., Hamada, M., Cristiano, L., Weidle, C. & Köhn, D. (2020), The slab puzzle of the Alpine-Mediterranean region: Insights from a new, high-resolution, shear wave velocity model of the upper mantle. *Geochemistry, Geophysics, Geosystems, 21*(8), e2020GC008993.

Faccenna, C., Becker, T.W., Auer, L., Billi, A., Boschi, L., Brun, J.P., Capitanio, F.A., Funiciello, F., Horvàth, F., Jolivet, L., Piromallo, C., Royden, L., Rossetti, F., Serpelloni, E. (2014), Mantle dynamics in the Mediterranean. *Reviews in Geophysics, 52*, 283–332. https://doi.org/10.1002/2013RG000444.Received

Fichtner, A., Villaseñor, A. (2015), Crust and upper mantle of the western Mediterranean - Constraints from full-waveform inversion. *Earth Planetary Science Letters, 428*, 52–62. https://doi.org/10.1016/j.epsl.2015.07.038

Fornelli, A., Gallicchio, S., Micheletti, F., & Langone, A. (2020), Preliminary U-Pb detrital zircon ages from Tufiti di Tusa formation (Lucanian Apennines, Southern Italy): Evidence of rupelian volcaniclastic supply. *Minerals, 10*(9), 786.

Frifita, N., Mickus, K., Gharbi, M. (2020), Gravity contribution to the Mejerda foreland basin, Northwestern region of Tunisia. *Journal of African Earth Science, 171*, 103956.

https://doi.org/https://doi.org/10.1016/j.jafrearsci.2020.103956.

Frizon de Lamotte, D., Andrieux, J. E. A. N., & Guezou, J. C. (1991), Cinematique des chevauchements neogenes dans l'Arc betico-rifain; discussion sur les modeles geodynamiques. *Bulletin de la Société géologique de France*, *162*(4), 611-626.

Frizon de Lamotte, D., Saint Bezar, B., Bracène, R., & Mercier, E. (2000), The two main steps of the Atlas building and geodynamics of the western Mediterranean. *Tectonics, 19*(4), 740-761.

Gaidi, S., Booth-Rea, G., Melki, F., Marzougui, W., Ruano, P., Pérez-Peña, J. V, Azañón, J.M., Zargouni, F., Chouaieb, H., Galve, J.P. (2020), Active fault segmentation in Northern Tunisia. J*ournal of Structural Geology, 139*, 104146. https://doi.org/https://doi.org/10.1016/j.jsg.2020.104146.

García-Dueñas, V., Balanyá, J. C., & Martínez-Martínez, J. M. (1992), Miocene extensional detachments in the outcropping basement of the northern Alboran basin (Betics) and their tectonic implications. *Geo-Marine Letters, 12*(2), 88-95.

Gartrell, A. P. (1997), Evolution of rift basins and low-angle detachments in multilayer analog models. *Geology, 25*(7), 615-618.

Gelabert, B., Sabat, F., & Rodríguez-Perea, A. (1992), A structural outline of the Serra de Tramuntana of Mallorca (Balearic Islands). *Tectonophysics*, *203*(1-4), 167-183.

Gerogiannis, N., Aravadinou, E., Chatzaras, V., & Xypolias, P. (2021), Calcite pseudomorphs after aragonite: A tool to unravel the structural history of high-pressure marbles (Evia Island, Greece). *Journal of Structural Geology, 148*, 104373.

Ghanmi, M., Youssef, M. Ben, Jouirou, M., Zargouni, F., Vila, J.M. (2001), " Glacier de sel" du Jebel Kebbouch (NW Tunisie). Eclogae Geol. Helv. 94, 153–160.

Ghanmi, M.A., Chaieb, A., Zaafouri, A., Salem, M.S. Ben, Aridhi, K., Ghanmi, M., Zargouni, F. (2019), Salt tectonics in the Maknassy-Mezzouna region of Tunisia: Example of intrusive and extrusive Triassic evaporites in the central and Southern Atlas. *Journal of African Earth Science, 158*, 103557.

Ghisetti, F., Vezzani, L. (2002), Normal faulting, extension and uplift in the outer thrust belt of the central Apennines (Italy): role of the Caramanico fault. *Basin Research, 14*, 225–236.

Ghorabi, M., Henry, B. (1992), Magnetic fabric of rock from Jebel Hairech (Northern Tunisia) and its structural implications. *Journal of African Earth Science (and Middle East) 14*, 267–

274. https://doi.org/https://doi.org/10.1016/0899-5362(92)90103-J

Globig, J., Fernàndez, M., Torne, M., Vergés, J., Robert, A., Faccenna, C. (2016), New insights into the crust and lithospheric mantle structure of Africa from elevation, geoid, and thermal analysis. J*ournal of Geophysical Research Solid Earth, 121*, 5389–5424.

Govers, R., Wortel, M.J.R. (2005), Lithosphere tearing at STEP faults: Response to edges of subduction zones. *Earth and Planetary Science letters, 236*, 505–523. https://doi.org/10.1016/j.epsl.2005.03.022

Guidotti, C. V, Sassi, F.P., 1986. Classification and correlation of metamorphic facies series by means of Muscovite b (o) data from low-grade metapelites. Neues Jahrb. für Mineral. Abhandlungen 153, 363–380.

Halloul, N., & Gourgaud, A. (2012), The post-collisional volcanism of northern Tunisia: petrology and evolution through time. *Journal of African Earth Sciences, 63*, 62-76.

Jabaloy, A., Galindo-Zaldivar, J. and Gonzalez-Lodeiro, F. (1993), The Alpujarride Nevado-Fibabride Extensional Shear Zone, Betic-Cordillera, SE Spain. *Journal of Structural Geology, 15*, 555-569.

Jallouli, C., Mickus, K. (2000), Regional gravity analysis of the crustal structure of Tunisia. *Journal of African Earth Science, 30*, 63–78.

Jemmali, N., Souissi, F., Carranza, E.J.M., Vennemann, T.W., Bogdanov, K. (2014), Geochemical constraints on the genesis of the Pb–Zn deposit of Jalta (northern Tunisia): Implications for timing of mineralization, sources of metals and relationship to the Neogene volcanism. *Geochemistry, 74*, 601–613.

Jimenez-Bonilla, A., Torvela, T., Balanyá, J. C., Expósito, I., & Díaz-Azpiroz, M. (2016), Changes in dip and frictional properties of the basal detachment controlling orogenic wedge propagation and frontal collapse: The external central Betics case. *Tectonics, 35*(12), 3028-3049.

Jolivet, L., Menant, A., Clerc, C., Sternai, P., Bellahsen, N., Leroy, S., Pik, R., Stab, M., Faccenna, C. & Gorini, C. (2018), Extensional crustal tectonics and crust-mantle coupling, a view from the geological record. *Earth-Science Reviews, 185*, 1187-1209.

Khelil, M., Souloumiac, P., Maillot, B., Khomsi, S., Frizon de Lamotte, D., 2019. How to build an extensional basin in a contractional setting ? Numerical and physical modelling applied to the Mejerda Basin at the front of the eastern Tell of Tunisia. *Journal of Structural*

Geology, 129, 103887. https://doi.org/10.1016/j.jsg.2019.103887

Kherroubi, A., Déverchère, J., Yelles, A., Mercier de Lépinay, B., Domzig, A., Cattaneo, A., Bracène, R., Gaullier, V., Graindorge, D. (2009), Recent and active deformation pattern off the easternmost Algerian margin, Western Mediterranean Sea: New evidence for contractional tectonic reactivation. *Marine Geology, 261*, 17–32. https://doi.org/https://doi.org/10.1016/j.margeo.2008.05.016

Khomsi, S., Ghazi, M., Jemia, B., Frizon, D., Lamotte, D., Maherssi, C., Echihi, O., Mezni, R., Ben Jemia, M.G., de Lamotte, D.F., Maherssi, C., Echihi, O., Mezni, R. (2009), An overview of the Late Cretaceous–Eocene positive inversions and Oligo-Miocene subsidence events in the foreland of the Tunisian Atlas: Structural style and implications for the tectonic agenda of the Maghrebian Atlas system. *Tectonophysics, 475*, 38–58. https://doi.org/10.1016/j.tecto.2009.02.027

Khomsi, S., Lamotte, D.F. De, Bédir, M., Echihi, O. (2016), The Late Eocene and Late Miocene fronts of the Atlas Belt in eastern Maghreb : integration in the geodynamic evolution of the Mediterranean Domain. *Arabian Journal of Geoscienc*e https://doi.org/10.1007/s12517-016-2609-1

Khomsi, S., Khelil, M., Roure, F., & Zargouni, F. (2021), Surface and subsurface architecture of the Kasseb structures: implications for petroleum exploration beneath the Tellian allochthon, the easternmost portion of the Maghrebides. *Arabian Journal of Geosciences, 14*(3), 1-20.

Kisch, H.J. (1991), Illite crystallinity: recommendations on sample preparation, X-ray diffraction settings, and interlaboratory samples. *Journal of Metamorphic Geology, 9*, 665–670.

Khomsi, S., Roure, F., & Vergés, J. (2022), Hinterland and foreland structures of the eastern Maghreb Tell and Atlas thrust belts: tectonic controlling factors, pending questions, and oil/gas exploration potential of the Pre-Triassic traps. *Arabian Journal of Geosciences*, *15*(6), 1-11.

Kurtz, J. (1983), Geochemistry of Early Mesozoic basalts from Tunisia. J*ournal of African Earth Sciences, 1*(2), 113-125.

Lanari, P., Wagner, T., & Vidal, O. (2014), A thermodynamic model for di-trioctahedral chlorite from experimental and natural data in the system MgO–FeO–Al2O3–SiO2–H2O: applications to P–T sections and geothermometry. Contributions to Mineralogy and

Petrology, 167(2), 1-19.

Leoni, L., Sartori, F., Tamponi, M. (1998), Composition variation in K-white micas and chlorites coexisting in Al-saturated metapelites under late diagenetic to low grade metamorphic conditions (Internal Liguride Units, Northern Apennines, Italy). *European Journal of Mineralogy, 10*, 1321–1339.

Leprêtre, R., Frizon de Lamotte, D., Combier, V., Gimeno-Vives, O., Mohn, G., & Eschard, R. (2018), The Tell-Rif orogenic system (Morocco, Algeria, Tunisia) and the structural heritage of the southern Tethys margin. *BSGF-Earth Sciences Bulletin, 189*(2), 10.

Levander, A., Bezada, M.J., Niu, F., Humphreys, E.D., Palomeras, I., Thurner, S.M., Masy, J., Schmitz, M., Gallart, J., Carbonell, R., Miller, M.S. (2014), Subduction-driven recycling of continental margin lithosphere. *Nature, 515*, 253–256. https://doi.org/10.1038/nature13878

Li, Q., Palomeras, I., & Meng, X. (2021), Lithospheric structure beneath southern Iberia and northern Morocco constrained by 3D Kirchhoff-approximate GRT imaging. *Journal of Geophysics and Engineering, 18*(2), 268-281.

Lonergan, L., & Platt, J. P. (1995), The Malaguide-Alpujarride boundary: a major extensional contact in the Internal Zone of the eastern Betic Cordillera, SE Spain. *Journal of Structural Geology, 17*(12), 1655-1671.

Lonergan, L., White, N. (1997), Origin of the Betic-Rif mountain belt. *Tectonics, 16*, 504–522. https://doi.org/10.1029/96TC03937

Lucazeau, F. (2019), Analysis and mapping of an updated terrestrial heat flow data set. *Geochemistry, Geophysics, Geosystems, 20*(8), 4001-4024.

Lucazeau, F., Dhia, H. Ben (1989), Preliminary heat-flow density data from Tunisia and the Pelagian Sea. *Canadian Journal of Earth Science, 2*6, 993–1000.

Mahdi, D., Abdallah, R. Ben, Hatira, N., Tlili, A., Chaftar, H.R., Jamoussi, F. (2013), Burial history determination of the Triassic succession of Central and Northern Tunisia using clay minerals. *Arabian Journal of Geoscience,* 6, 4347–4355.

Malusà, M. G., Faccenna, C., Baldwin, S. L., Fitzgerald, P. G., Rossetti, F., Balestrieri, M. L., Danisík, M., Ellero, A., Ottria, G. & Piromallo, C. (2015), Contrasting styles of (U) HP rock exhumation along the Cenozoic Adria-Europe plate boundary (Western Alps, Calabria, Corsica). *Geochemistry, Geophysics, Geosystems, 16*(6), 1786-1824.

Mancilla, F. de L., & Diaz, J. (2015), High resolution Moho topography map beneath Iberia and

Northern Morocco from receiver function analysis. *Tectonophysics, 663*, 203-211.
Mancilla, F. de L., Booth-Rea, G., Stich, D., Pérez-Peña, J.V., Morales, J., Azañón, J.M., Martin, R., Giaconia, F. (2015), Slab rupture and delamination under the Betics and Rif constrained from receiver functions. *Tectonophysics, 663*, 225–237. https://doi.org/https://doi.org/10.1016/j.tecto.2015.06.028
Martínez-Martínez, J.M., Booth-Rea, G., Azañón, J.M., Torcal, F. (2006), Active transfer fault zone linking a segmented extensional system (Betics, southern Spain): Insight into heterogeneous extension driven by edge delamination. *Tectonophysics, 422*, 159–173. https://doi.org/https://doi.org/10.1016/j.tecto.2006.06.001
Martínez-Martínez, J.M., Soto, J.I., Balanyá, J.C. (2002), Orthogonal folding of extensional detachments: structure and origin of the Sierra Nevada elongated dome (Betics, SE Spain). *Tectonics, 21*, 1–3.
Marzougui, W., Melki, F., Arfaoui, M., Houla, Y., Zargouni, F. (2015), Major faults, salt structures and paleo-ridge at tectonic nodes in Northern Tunisia: contribution of tectonics and gravity analysis. *Arabian Journal of Geoscience, 8*, 7601-7617.
Massonne, H.J., Schreyer, W. (1987), Phengite geobarometry based on the limiting assemblage with K-feldspar, phlogopite and quartz. *Contributions to Mineralogy and Petrology, 96*, 214–224.
Massonne, H.J., Szpurka, Z. (1997), Thermodynamic properties of white micas on the basis of high-pressure experiments in the systems K2O-MgO-Al2O3-SiO2-H2O. *Lithos, 41*, 229–250.
Masrouhi, A., Ghanmi, M., Slama, M. M. B., Youssef, M. B., Vila, J. M., & Zargouni, F. (2008), New tectono-sedimentary evidence constraining the timing of the positive tectonic inversion and the Eocene Atlasic phase in northern Tunisia: implication for the North African paleo-margin evolution. *Comptes Rendus Geoscience, 340*(11), 771-778.
Masrouhi, A., Bellier, O., Koyi, H. (2014), Geometry and structural evolution of Lorbeus diapir , northwestern Tunisia : polyphase diapirism of the North African inverted passive margin. *International Journal of Earth Science, 103*, 881–900. https://doi.org/10.1007/s00531-013-0992-3
Masrouhi, A., Koyi, H.A. (2012), Submarine 'salt glacier' of Northern Tunisia, a case of Triassic salt mobility in North African Cretaceous passive margin. *Geological Society of London*

Special Publications, 363, 579–593. https://doi.org/10.1144/sp363.29

Melki, F., Zouaghi, T., Chelbi, M. Ben, Bédir, M., Zargouni, F. (2010), Tectono-sedimentary events and geodynamic evolution of the Mesozoic and Cenozoic basins of the Alpine Margin, Gulf of Tunis, north-eastern Tunisia offshore. *Comptes Rendus Geoscience, 342*, 741–753. https://doi.org/10.1016/j.crte.2010.04.005

Melki, F., Zouaghi, T., Harrab, S., Sainz, A.C., Bédir, M., Zargouni, F. (2011), Structuring and evolution of Neogene transcurrent basins in the Tellian foreland domain, north-eastern Tunisia. Journal of Geodynamics, 52, 57–69.

Merriman, R.J., Peacor, D.R. (1998), Very low-grade metapelites: mineralogy, microfabrics and measuring reaction progress. *Low-grade Metamorphism,* 10–60.

Merriman, R.J., Roberts, B. (1985), A survey of white mica crystallinity and polytypes in pelitic rocks of Snowdonia and Llŷn, North Wales. *Mineralogical Magazine, 49*, 305–319.

Miller, M. S., & Agostinetti, N. P. (2012), Insights into the evolution of the Italian lithospheric structure from S receiver function analysis. *Earth and Planetary Science Letters, 345*, 49-59.

Moragues, L., Rea, G.B., Ruano, P., Azañón, J.M., Gaidi, S., Peña, J.V.P. (2018), Middle Miocene extensional tectonics in southeast Mallorca Island (Western Mediterranean). Revista de la Sociedad Geológica de España, *31*(2), 101-110.

Morales, J., Molina-Aguilera, A., de Lis Mancilla, F., Stich, D., Azañón, J. M., Teixidó, T., López-Comino, J.A., Heit, B., Yuan, X. & Posadas, A. M. (2022), Preservation of the Iberian Tethys paleomargin beneath the eastern Betic mountain range. *Gondwana Research, 106*, 237-246.

Morata, D., Aguirre, L., Puga, E. (1994), Na-metamorphic pyroxenes in low-grade metabasites from the External Zones of the Betic Cordilleras (southern Spain): influence of rock chemical composition on their formation. *Andean Geology, 21*, 269–283.

Morgan, P., James, D.E. (1989), *Heat flow in the earth. Encyclopedia of Solid Earth Geophysics*. Van Nostrand Reinhold, New York 634–646.

Naouali, B.S., Guellala, R., Bey, S., Inoubli, M.H. (2017), Gravity data contribution for petroleum exploration domain: Mateur case study (Saliferous Province, Northern Tunisia). *Arabian Journal for Science and Engineering, 42*, 339–352.

Negro, F., Agard, P., Goffe, B., Saddiqui, O. (2007), Tectonic and metamorphic evolution of the

Temsamane units , External Rif (northern Morocco): implications for the evolution of the Rif and the Betic – Rif arc. *Journal of the Geological Society, 164*, 829–842.

Nieto, F. (1997), Chemical composition of metapelitic chlorites; X-ray diffraction and optical property approach. *European Journal of Mineralogy, 9*, 829–841.

Nieto, F., Mata, M.P., Bauluz, B., Giorgetti, G., Arkai, P., Peacor, D.R. (2005), Retrograde diagenesis, a widespread process on a regional scale. *Clay Minerals, 40*, 93–104.

Nocquet, J. (2012), Present-day kinematics of the Mediterranean : A comprehensive overview of GPS results. *Tectonophysics, 579*, 220–242. https://doi.org/10.1016/j.tecto.2012.03.037

Palomeras, I., Thurner, S., Levander, A., Liu, K., Villaseñor, A., Carbonell, R., & Harnafi, M. (2014), Finite-frequency Rayleigh wave tomography of the western Mediterranean: Mapping its lithospheric structure. *Geochemistry, Geophysics, Geosystems, 15*(1), 140-160.

Papeschi, S., Musumeci, G., & Mazzarini, F. (2017), Heterogeneous brittle-ductile deformation at shallow crustal levels under high thermal conditions: The case of a synkinematic contact aureole in the inner northern Apennines, southeastern Elba Island, Italy. *Tectonophysics, 717*, 547-564.

Paton, C., Hellstrom, J., Paul, B., Woodhead, J. and Hergt J. (2011), Iolite: Freeware for the visualisation and processing of mass spectrometric data. *Journal of Analytical Atomic Spectrometry, 26*(12), 2508-2518, doi:10.1039/c1ja10172b.

Perthuisot, V., 1981. Diapirism in northern Tunisia. *Journal of Structural Geology, 3*, 231–235.

Petit, C., Le Pourhiet, L., Scalabrino, B., Corsini, M., Bonnin, M., & Romagny, A. (2015), Crustal structure and gravity anomalies beneath the Rif, northern Morocco: implications for the current tectonics of the Alboran region. *Geophysical Journal International, 202*(1), 640-652.

Piana Agostinetti, N., Lucente, F. P., Selvaggi, G., & Di Bona, M. (2002), Crustal structure and Moho geometry beneath the Northern Apennines (Italy). *Geophysical Research Letters, 29*(20), 60-1.

Piromallo, C., Morelli, A. (2003), *P* wave tomography of the mantle under the Alpine-Mediterranean area. *Journal of Geosphysical Research Solid Earth, 108*, 1–23. https://doi.org/10.1029/2002JB001757

Platt, J. P. (1986), Dynamics of orogenic wedges and the uplift of high-pressure metamorphic rocks. *Geological Society of America Bulletin, 97*(9), 1037-1053.

Puga, E., de Fliert, V., Torres-Roldán, R.L., Sanz de Galdeano, C. (1988), Attempts of whole-rock K/Ar dating of Mesozoic volcanic and hypabissal igneous rocks from the Central Subbetic (Southern Spain): A case of differential Argon loss related to very low-grade metamorphism. *Estudios Geológicos, 44*(1-2): 47-59

Rabaute, A., Chamot-Rooke, N. (2014), Active tectonics of the Africa–Eurasia boundary from Algiers to Calabria, map at 1:1500 000 scale with GIS database. Geosubsight, Paris.

Radi, Z., Yelles-Chaouche, A., Corchete, V., Guettouche, S. (2017), Crust and upper mantle shear wave structure of Northeast Algeria from Rayleigh wave dispersion analysis. *Physics of the Earth and Planetary Interiors, 270*, 84–89.

Ramzi, A., Lassaad, C. (2017), Superposed folding in the Neogene series of the northeastern Tunisia : precision of the upper Miocene compression and geodynamic significance. *International Journal of Earth Science, 106*, 1905–1918. https://doi.org/10.1007/s00531-016-1394-0

Research group for lithospheric structure in Tunisia (1992), The EGT´85 seismic experiment in Tunisia: a reconnaissance of the deep structures. *Tectonophysics, 207*, 245–267.

Riahi, S., Soussi, M., & Stow, D. (2021), Sedimentological and stratigraphic constraints on Oligo–Miocene deposition in the Mogod Mountains, northern Tunisia: new insights for paleogeographic evolution of North Africa passive margin. *International Journal of Earth Sciences, 110*(2), 653-688.

Röder, G. (1988), Numidian Marble and Some of its Specialities, in: Herz, N., Waelkens, M. (Eds.), *Classical Marble: Geochemistry, Technology, Trade*. Springer Netherlands, Dordrecht, pp. 91–96. https://doi.org/10.1007/978-94-015-7795-3_10

Rodríguez-Fernández, J., Azor, A., & Miguel Azañón, J. (2011), The Betic intramontane basins (SE spain): stratigraphy, subsidence, and tectonic history. In: Busby, C. and Azor, A. (Eds), *Tectonics of sedimentary basins: Recent advances*, 461-479. https://doi.org/10.1002/9781444347166.ch23

Rodríguez-Fernández, J., Roldán, F.J., Azañón, J.M., García-Cortés, A. (2013), El colapso gravitacional del frente orogénico alpino en el Dominio Subbético durante el Mioceno medio-superior: El Complejo Extensional Subbético. *Boletín Geológico y Minero, 124*, 477–504.

Romagny, A., Jolivet, L., Menant, A., Bessière, E., Maillard, A., Canva, A., Gorini, C. & Augier,

R. (2020), Detailed tectonic reconstructions of the Western Mediterranean region for the last 35 Ma, insights on driving mechanismsReconstructions détaillées de la Méditerranée occidentale depuis 35 Ma, implications en terme de mécanismes moteur. *BSGF-Earth Sciences Bulletin, 191*(1), 37.

Roure, F., Casero, P., Addoum, B. (2012), Alpine inversion of the North African margin and delamination of its continental lithosphere. *Tectonics, 31*, 1–28. https://doi.org/10.1029/2011TC002989

Rouvier, H. (1993), *Carte géologique de la Tunisie au 1/50.000*, la feuille n◦ 24 de Fernena.Tunis, Tunisie. Office National des Mines.

Rouvier, H. (1992), Carte géologique de la Tunisie au 1/50.000, la feuille n◦ 19 d'Ain Drahem.Tunis, Tunisie. Office National des Mines.

Rouvier, H. (1977), Gelogie de l'Extreme-Nord tunisien: tectoniques et paleogeographies superposees a l'extremite orientale de la chaine nord-maghrebine. These Dr. es Sc., Univ. Pierre Marie Curie.

Rubatto, D., Gebauer, D., & Fanning, M. (1998), Jurassic formation and Eocene subduction of the Zermatt–Saas-Fee ophiolites: implications for the geodynamic evolution of the Central and Western Alps. *Contributions to Mineralogy and Petrology, 132*(3), 269-287.

Sàbat, F., Gelabert, B., Rodríguez-Perea, A., & Giménez, J. (2011), Geological structure and evolution of Majorca: Implications for the origin of the Western Mediterranean. *Tectonophysics, 510*(1-2), 217-238.

Saïd, A., Baby, P., Chardon, D., Ouali, J. (2011), Structure, paleogeographic inheritance, and deformation history of the southern Atlas foreland fold and thrust belt of Tunisia. *Tectonics, 30 (6).* https://doi.org/10.1029/2011TC002862.

Saïd, A., Chardon, D., Baby, P., Ouali, J. (2011), Active oblique ramp faulting in the Southern Tunisian Atlas. *Tectonophysics, 499*, 178–189. https://doi.org/10.1016/j.tecto.2011.01.010

Salaj, J., & Vanhouten, F. B. (1988), Cenozoic Paleogeographic development of northern Tunisia, with special reference to the stratigraphic record in the Miocene trough. *Palaeogeography, Palaeoclimatology, Palaeoecology, 64*(1–2), 43–57. https://doi.org/10.1016/0031-0182(88)90141-1

Sami, R., Soussi, M., Kamel, B., Kmar, B. I. L., Stow, D., Sami, K., & Mourad, B. (2010), Stratigraphy, sedimentology and structure of the Numidian Flysch thrust belt in northern

Tunisia. *Journal of African Earth Sciences, 57*(1-2), 109-126.

Sassi, F.P., Scolari, A. (1974), The bo value of the potassium white micas as a barometric indicator in low-grade metamorphism of pelitic schits. *Contributions to Mineralogy and Petrology, 45*, 143–152.

Schmitz, M. D. and Schoene B. (2007), Derivation of isotope ratios, errors, and error correlations for U-Pb geochronology using 205Pb-235U-(233U)-spiked isotope dilution thermal ionization mass spectrometric data. *Geochemistry, Geophysics, Geosystems, 8*(Q08006), doi:doi.org/10.1029/2006GC001492.

Soumaya, A., Ben Ayed, N., Delvaux, D., Ghanmi, M. (2015), Spatial variation of present-day stress field and tectonic regime in Tunisia and surroundings from formal inversion of focal mechanisms: Geodynamic implications for central Mediterranean. *Tectonics, 34*, 1154–1180. https://doi.org/10.1002/2015TC003895

Soumaya, A., Kadri, A., Ben Ayed, N., Kim, Y.-S., Dooley, T.P., Rajabi, M., Braham, A. (2020), Deformation styles related to intraplate strike-slip fault systems of the Saharan-Tunisian Southern Atlas (North Africa): New kinematic models. J*ournal of Structural Geology, 104175*. https://doi.org/https://doi.org/10.1016/j.jsg.2020.104175

Platt, J. P., Allerton, S., Kirker, A., Mandeville, C., Mayfield, A., Platzman, E. S., & Rimi, A. (2003), The ultimate arc: Differential displacement, oroclinal bending, and vertical axis rotation in the External Betic-Rif arc. *Tectonics*, *22*(3).

Trincal, V., Lanari, P., Buatier, M., Lacroix, B., Charpentier, D., Labaume, P., & Muñoz, M. (2015), Temperature micro-mapping in oscillatory-zoned chlorite: Application to study of a green-schist facies fault zone in the Pyrenean Axial Zone (Spain). *American Mineralogist*, *100*(11-12), 2468-2483.

Troudi, H., Tari, G., Alouani, W., Cantarella, G. (2017), Styles of Salt Tectonics in Central Tunisia : An Overview. In: *Permo-Triassic Salt Provinces of Europe, North Africa and the Atlantic Margins: Tectonics and Hydrocarbon Potential*. Elsevier Inc. https://doi.org/10.1016/B978-0-12-809417-4.00026-4

Van Hinsbergen, D.J.J., Vissers, R.L.M., Spakman, W. (2014), Origin and consequences of western Mediterranean subduction, rollback, and slab segmentation. *Tectonics, 33*, 393-419. https://doi.org/10.1002/2013TC003349

Van Hinsbergen, D. J., Torsvik, T. H., Schmid, S. M., Maţenco, L. C., Maffione, M., Vissers, R. L., Gürer, D. & Spakman, W. (2020), Orogenic architecture of the Mediterranean region and kinematic reconstruction of its tectonic evolution since the Triassic. *Gondwana Research, 81*, 79-229.

Vázquez, M., Asebriy, L., Azimousa, A., Jabaloy, A., Booth-Rea, G., Barbero, L., Mellini, M. & González-Lodeiro, F. (2013), Evidence of extensional metamorphism associated to Cretaceous rifting of the North-Maghrebian passive margin: The Tanger-Ketama Unit (External Rif, northern Morocco). *Geologica Acta, 11*(3), 277-293.

Vermeesch, P. (2018), IsoplotR: A free and open toolbox for geochronology. *Geoscience Frontiers, 9*(5), 1479-1493, doi:10.1016/j.gsf.2018.04.001.

Vidal, O., Parra, T. (2000), Exhumation paths for high pressure metapelites obtained from local equilibria for chlorite–phengite assemblages. *Geological Journal, 35*, 139–161.

Vidal, O., Parra, T., Trotet, F. (2001), A thermodynamic model for Fe-Mg aluminous chlorite using data from phase equilibrium experiments and natural pelitic assemblages in the 100-600 ºC, 1-25 kbar P-T range. *American Journal of Sciences, 301*, 557-592.

Vidal, O., Parra, T., Vieillard, P. (2005), Thermodynamic properties of the Tschermak solid solution in Fe-chlorite: Application to natural examples and possible role of oxidation. *American Mineralogist, 90*, 347-358.

Vidal, O., Lanari, P., Muñoz, M., Bourdelle, F., de Andrade, V. (2016), Deciphering temperature, pressure and oxygen-activity conditions of chlorite formation. *Clay Minerals, 51*, 615–633. https://doi.org/10.1180/claymin.2016.051.4.06

Vila et al. (1996), A large submarine middle Albian "'salt glacier'" in north-western Tunisia (250 km(2): The Triassic rocks of Ben Gasseur "diapir'" and of El Kef anticline. *Comtes Rendus de l´Academie des Sciences Serie II A 322*(3), 221–227.

Vila, J.M. (1995), First Terrestrial Study of a Large Submarine Salt Glacier - the Eastern Part of the Ouenza-Ladjebel-Meridef Structure (Algerian Tunisian Confines) - Proposal for an Emplacement Scenario and Comparisons. B Soc Geol Fr 166(2), 149–167.

Villa, I. M., Bucher, S., Bousquet, R., Kleinhanns, I. C., & Schmid, S. M. (2014), Dating polygenetic metamorphic assemblages along a transect across the Western Alps. *Journal of Petrology, 55*(4), 803-830.

Warr, L.N., Ferreiro-Mahlmann, R. (2015), Recommendations for Kübler Index standardization.

Clay Miner. 50, 283–286. https://doi.org/10.1180/claymin.2015.050.3.02

Warr, L.N., Rice, A.H.N. (1994), Interlaboratory standardization and calibration of clay mineral crystallinity and crystallite size data. *Journal of Metamorphic Geology, 12*, 141–152.

Wernicke, B. (1981), Low-angle normal faults in the Basin and Range Province: nappe tectonics in an extending orogen. *Nature, 291*(5817), 645-648.

Wernicke, B., & Burchfiel, B. C. (1982), Modes of extensional tectonics. *Journal of Structural Geology, 4*(2), 105-115.

Wortel, M. J. R., & Spakman, W. (2000), Subduction and slab detachment in the Mediterranean-Carpathian region. *Science, 290*(5498), 1910-1917.

Yans, J., Verhaert, M., Gautheron, C., Antoine, P. O., Moussi, B., Dekoninck, A., Chaftar, H.-R., Hatira, N., Dupuis, C., Pinna-Jamme, R. & Jamoussi, F. (2021), (U-Th)/He Dating of Supergene Iron (Oxyhydr-) Oxides of the Nefza-Sejnane District (Tunisia): New Insights into Mineralization and Mammalian Biostratigraphy. *Minerals, 11*(3), 260.

Zouaghi, T., Bédir, M., Ayed-Khaled, A., Lazzez, M., Soua, M., Amri, A., Inoubli, M.H. (2013), Autochthonous versus allochthonous Upper Triassic evaporites in the Sbiba graben, central Tunisia. *Journal of Structural Geology, 52*, 163–182.

Sample	Spot	207Pb/235U	07/35 Err [2 S.E]	206Pb/238U	06/38 Err [2 S.E]	(rho)	238U/206Pb	38/06 - Err [2 S.E]	207Pb/206Pb	07/06 Err [2 S.E.]	(rho)2	U ppm	2SD U ppm	Pb ppm	2SD Pb ppm
Ghzele-b	1	1.47	0.17	0.0221	0.00115	0.68078	45.24887	2.354579	0.468	0.0425	-0.2455	11.9	0.5	690	30
Ghzele-b	2	0.266	0.034	0.0096	0.00055	-0.2034	104.1667	5.96788	0.189	0.0255	0.44137	11.8	0.19	119	11.5
Ghzele-b	3	0.163	0.022	0.0094	0.00055	0.068435	106.383	6.224535	0.123	0.019	0.043445	9.85	0.185	34	3.75
Ghzele-b	4	0.238	0.0345	0.0101	0.0006	0.012238	99.0099	5.881775	0.2	0.032	0.98659	9.5	0.26	52	5.75
Ghzele-b	5	0.52	0.06	0.0149	0.0009	-0.24855	67.11409	4.0538715	0.287	0.043	0.61928	7	0.135	75	5.25
Ghzele-b	6	0.326	0.038	0.0115	0.0007	0.12463	86.95652	5.293005	0.25	0.034	0.85297	6.99	0.2	66	5
Ghzele-b	7	0.479	0.0325	0.0113	0.0007	0.051911	88.49558	5.482025	0.315	0.0295	0.79708	14.11	0.305	287	13.5
Ghzele-b	8	1.34	0.135	0.022	0.0014	0.38136	45.45455	2.892562	0.48	0.05	0.67507	6.63	0.245	188	8.25
Ghzele-b	9	0.77	0.08	0.017	0.0011	0.431	58.82353	3.8062285	0.315	0.032	0.28426	6.81	0.24	178	8.75
Ghzele-b	10	0.43	0.06	0.0107	0.0007	0.43247	93.45794	6.11407	0.3	0.044	0.33791	7.87	0.13	94	10
Ghzele-b	11	0.252	0.0335	0.0114	0.00075	-0.055214	87.7193	5.771005	0.217	0.045	0.99725	10.54	0.17	68	5.75
Ghzele-b	12	0.213	0.0395	0.0105	0.0007	0.23828	95.2381	6.349205	0.167	0.032	0.76363	9.72	0.275	34	3
Ghzele-b	13	0.415	0.045	0.0134	0.0009	0.050977	74.62687	5.01225	0.268	0.034	0.50867	11.49	0.31	129	8.75
Ghzele-b	14	1.12	0.11	0.0225	0.00155	0.55705	44.44444	3.0617285	0.396	0.035	0.42493	7.77	0.15	312	17
Ghzele-b	15	0.193	0.0375	0.0107	0.00075	0.18332	93.45794	6.55079	0.15	0.03	0.54431	12.83	0.17	30	3.75
Ghzele-b	16	0.169	0.0305	0.0098	0.0007	-0.11352	102.0408	7.28863	0.124	0.0275	0.43411	11.07	0.225	28	3.5
Ghzele-b	17	0.85	0.055	0.0195	0.00145	0.084165	51.28205	3.8132805	0.363	0.0325	0.046368	10.43	0.27	214	13
Ghzele-b	18	0.236	0.047	0.0116	0.0009	-0.077488	86.2069	6.688465	0.2	0.055	0.99614	7.33	0.16	17.2	2.325
Ghzele-b	19	0.353	0.0375	0.0122	0.00095	0.025134	81.96721	6.382695	0.236	0.034	0.76998	12.26	0.175	195	8.75
Ghzele-b	20	0.272	0.0365	0.0101	0.0008	0.3203	99.0099	7.84237	0.183	0.027	0.3722	8.39	0.135	28	2.75
Ghzele-b	21	0.7	0.075	0.016	0.0013	0.41586	62.5	5.078125	0.336	0.041	0.92948	7.22	0.21	230	14.25
Ghzele-b	22	0.303	0.0475	0.0097	0.0008	0.16482	103.0928	8.5025	0.181	0.0345	0.4358	6.83	0.135	70	6.75
Ghzele-b	23	0.58	0.075	0.0148	0.00125	0.98541	67.56757	5.70672	0.26	0.0255	0.45485	7.56	0.27	94	7.25
Ghzele-b	24	0.26	0.05	0.0115	0.001	-0.042108	86.95652	7.561435	0.19	0.043	0.4664	5.62	0.095	32	3.5

Ghzele-b	25	0.54	0.075	0.0161	0.0017	0.56443	62.1118	6.55839	0.297	0.033	0.29876	10.9	1.1	187	11.5